

Dear editor,

We thank the two Referees for their valuable comments on our manuscript “Laboratory and field evaluation of the Aerosol Dynamics Inc. concentrator (ADIC) for aerosol mass spectrometry”. We think that the revision we made to the manuscript, based on the comment of the Reviewers, has improved the quality of the manuscript significantly. Most of the changes suggested by the Referees were implemented by adding requested technical details to the manuscript but we also added two figures to Supplemental material. In addition, some minor changes has been made throughout the manuscript to improve the grammar. All the changes to the manuscript have been made by “Track changes” mode and the changes in Supplemental information have been highlighted in yellow. Additionally, point-by-point responses to the comments of the Referees are given in separate author’s responses.

On behalf of all authors,

Sanna Saarikoski

Authors' response to Referee #1 comments

We would like to thank Referee #1 for the valuable comments that aided us to improve the manuscript. In this post, we will provide our response to the Referee's comments. In our replies, we provide original comment from the Referee and our response followed by the changes made to the manuscript.

General comment:

(1) More details on the physical aspects of the ADIc may need to be reported. For example, it would be helpful to know the dimensions of the ADIc growth tube and the residence time of particles for a certain flow rate. Also, for the sake of clarity, consider to add on Figure 1 references to the parameters reported in Table 1. In mentioning the importance of minimizing the time the particle being a droplet inside the growth tube (line 113), it would be useful to quote the approximate time scale. In addition, the issue whether the ADIc modifies the shape or phase of particles should be addressed, at least briefly. Such changes could significantly affect aerosol quantification by the AMS.

Response and author's changes in manuscript:

Dimensions: The dimensions of the growth tube are already stated in the manuscript (see the text starting on line 126 (page 5) "The conditioner, initiator and moderator are 140 mm, 51 mm and 102 mm long, respectively, separated by 7.5 mm thick insulator sections. In both prototypes the growth tube was lined with a 9 mm-ID, ~1.5 mm-thick wick formed from rolled membrane filter."

Residence Time: We added to the manuscript: "For particles along the centerline of the flow, the calculated residence time from the point of activation to the inlet of the focusing nozzle is 200-300 ms, depending on the point of activation. Along the flow trajectory that encompasses 50% of the flow, the residence time is as long as 400 ms."

Operating temperatures for conditioner, initiator, moderator and focusing nozzle have been added to Fig. 1.

Particle Shape: Discussion of particle shape has been added to manuscript (see details in response to comment 6).

Detailed comments:

(2) Line 18, change "ultrafine" to "fine" since ADIc can clearly concentrate particles beyond the ultrafine mode.

Response and author's changes in manuscript: "ultrafine" has been changed to "fine"

(3) Figure 2 shows the size dependent concentration factors for particles only up to 400 nm in mobility diameter. What are the concentration factors for larger particles? Also, the blue circles appear to show in two different shades. Are these from two separate sets of experiments? If so, explain the differences.

Response and author's changes in manuscript: Unfortunately we were not able to investigate the concentration factors for the particles larger than 400 nm (in mobility diameter) in the laboratory due to the instrumentation available. However, based on the ambient size distribution data measured by the SP-AMS at SMEAR III (Fig. 5), the CFs were rather stable until 1 μm in vacuum diameter (dva) corresponding to ~600 nm in mobility diameter (see figure below).

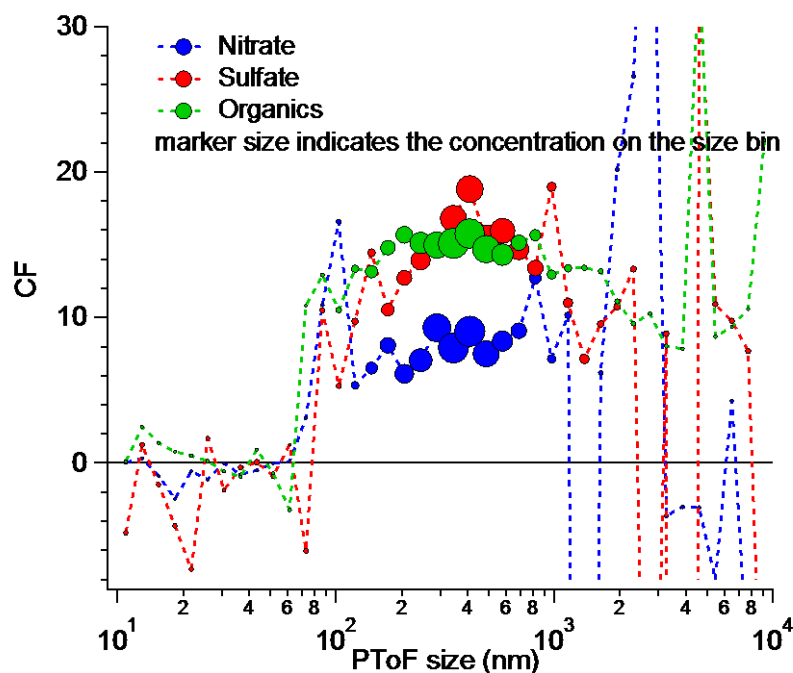


Fig. R1. Size dependent concentration factor for nitrate, sulfate and organics during the field measurements at SMEAR III in Helsinki.

In contrast, during the field measurements at ARI, the size distributions for organics and m/z 57 from the Q-AMS+ADIC were missing mass above $d_{va} \sim 700$ nm that was measured by the HR-AMS without the ADIC. This difference can be at least partly explained by a difference in the cutoff of the aerodynamic lenses in the two AMS instruments. The difference in the size distributions is discussed also in comment (7) for Referee #2.

All blue circles are from the same experiments so they should appear in same color.

No changes were made to manuscript based on this comment.

(4) Line 201, the sentence “. . . measured size distributions were normalized to the mass spectra” is vague. Consider to revise.

Response and author’s changes in manuscript: The sentence was modified to: “The measured size distributions were normalized to the mass concentrations measured in the mass spectrum mode.”

(5) Line 237, how often was SP-AMS switching between laser-on and laser-off?

Response and author’s changes in manuscript: Laser was switching between on and off every 1.5 minutes. Switching period has been added to manuscript.

(6) For the evaluation of ADIC’s influence on aerosol composition and size, Figure 4 is presented to compare the average high resolution mass spectra for organics and rBC from an SP-AMS downstream and bypass the ADIC. The measured-CF for Cx was significantly higher than for the other ions. Could it be due to change in particle shape, thus particle collection efficiency in the laser beam? It would be also interesting to see an evaluation of the ADIC’s influence on bulk PM composition, including both inorganics and organics.

Response and author’s changes in manuscript: The influence of ADIC on particle shape has been added to the text: “One possible explanation is that the ADIC altered the shape of the rBC-containing particles. The effect of the condensation/evaporation process on particle shape was not explored in

this study; however, others have found changes in the shape of aggregates. In a study using a condensation system similar to that employed here, Ma et al (2013) reported collapse of the aggregate structure of laboratory-generated soot in the evaporation process. Regarding the SP-AMS, the morphology of the particles had been demonstrated to affect the collection efficiency since it affects the overlap of the particle beam and the laser beam (Willis et al., 2014)."

The bulk PM composition measured by the SP-AMS with and without the ADIc has been added to Supplemental material (Fig. S4).

References

Ma, X., Zangmeister, C. D., Gigault, J., Mulholland, G. W., & Zachariah, M. R. (2013). Soot aggregate restructuring during water processing. *Journal of Aerosol Science*, 66, 209-219.

Willis, M.D., Lee, A.K.Y., Onasch, T.B., Fortner, E.C., Williams, L.R., Lambe, A.T., Worsnop, D.R., Abbatt, J.P.D., 2014. Collection efficiency of the soot-particle aerosol mass spectrometer (SP-AMS) for internally mixed particulate black carbon. *Atmos. Meas. Tech.* 7, 4507–4516.

(7) Line 311 – 313, this sentence is a bit confusing. Consider to revise.

Response and author's changes in manuscript: That sentence has been modified as well as few other sentences related to it.

(8) Line 355 – 358, does it mean that the Q-AMS and the SP-AMS report different ammonium concentration for the same air mass? Won't this discrepancy correctable through proper relative ionization efficiency calibration and fragmentation table adjustment (e.g., for better ammonium quantification)?

Response and author's changes in manuscript: The referee is correct that we did not have good agreement in bypass for ammonium between the Q-AMS and the HR-AMS, even with several RIE calibrations and adjustments to the fragmentation tables. Part of the problem is that ammonium concentration was low ($< 0.4 \text{ ug m}^{-3}$), and it was often close to the detection limit for the Q-AMS during the bypass periods. We think that this is an indication of how hard it is to get two instruments to agree for all species.

Lines 355-358 were revised:

"Another possibility is that the RIE for ammonium was incorrect for one or both of the instruments, even though it was measured before and after the ambient sampling period with pure AN particles. The CF during bypass periods was 1.3 ± 0.4 (Table 3) indicating that the two instruments did not agree well for ammonium even when the Q-AMS was bypassing the ADIc. However, the ammonium mass loading was low ($< 0.4 \text{ ug m}^{-3}$) and often close to the detection limit for the Q-AMS during the bypass periods, leading to a large uncertainty in the bypass CF."

(9) Fig 8, the ammonium measurement after ADIc shows more spikes. Is this an artifact induced by the ADIc?

Response and author's changes in manuscript: Ammonium spikes in the time series of the ACSM are not induced by the ADIc since similar spikes are seen in Fig. 9a when the ACSM was used in bypass without the ADIc. We think that these spikes are likely related to the detection of small air bubbles in the ACSM that affect the measured ammonium concentration. The spikes may be either negative or positive if the air bubble is released during the filter or aerosol measurement phase.

We added to figure caption 8: “Spikes in the time series of ammonium in the ACSM are likely related to the detection of small air bubbles in the ACSM that affect the measured ammonium concentration.”

Authors' response to Referee #2 comments

We would like to thank Referee #2 for the constructive comments that helped us to improve the manuscript. In this post, we will provide our response to the Referee's comments. In our replies, we provide original comment from the Referee and our response followed by the changes made to the manuscript.

(1) Lines 34-35, The sentence ". . .did not change the size distribution or the chemistry of the ambient aerosol particles." is too strong. The results do suggest there are some minor changes to the particle chemical composition (due to the composition dependence of concentration factor).

Response and author's changes in manuscript: sentence is now ...did not significantly change the size distribution...

(2) Please add diagrams illustrating the setup of the laboratory and field tests (at least in the supplementary information).

Response and author's changes in manuscript: Set-ups for the laboratory and fields test have been added to Supplemental information (Fig. S2).

(3) Please clarify what a "multiplex chopper" is.

Response and author's changes in manuscript: multiplex chopper is an efficient Particle time of Flight (ePToF) chopper that is based on a multiplexed particle beam chopper system with 50% particle throughput providing significantly improved signal-to-noise for the particle size measurement (compared to standard 1–2% throughput). We added to the text: ..."efficient Particle Time of Flight, ePToF, chopper) with 50% particle throughput."

(4) Line 270: how was CF measured? Fig. S2a-b shows the CF was 6.8 instead of 5.7.

Response and author's changes in manuscript: The CF of 5.7 was an average of the CFs calculated separately to each data point (n=652) while the CF based on the regression slope was 6.8. We think that the average of the CFs is a better representation of the data since the regression slope can be biased by the large values. In addition, it gives a more realistic uncertainty. We have changed the text to read:

"For the lower flow regime data (Fig. S3a–b), the average CF, calculated as the ratio of the number concentration in the output flow to that in the sample flow, was 5.7 ± 0.4 with a theoretical CF of 7.5. Linear regression of that data yielded a correlation coefficient (R^2) of 0.984. In the higher flow regime (Fig. S3c–d), the measured CF was 9.0 ± 0.7 , with a theoretical CF of 13.6."

(5) Figure S2c-d, the values of regression slope listed in Figures S2c and S2d are different (9.7 and 10.4).

Response and author's changes in manuscript: The correct regression slope in Fig. S2c (now Fig. S3c) is 10.4. The figure has been changed.

(6) Line 302, how frequently was the sampling alternated between ADIc and the bypass line?

Response and author's changes in manuscript: The SP-AM was switching between the bypass line and the ADIc every 30 minutes. Switching period has been added to the text.

(7) Lines 368-369: The low particle transmission efficiency through the lens is unlikely the only cause for the low CF. Figure S3c shows that in the lower size range (e.g., 400- 600 nm), the CF was about 5, substantially

below the theoretical value. How do the measurements of Q-AMS with ADIc bypassed compare with HR-AMS data for different species?

Response and author's changes in manuscript: The referee is right that the CF for organics and m/z 57 (~ 6 and ~ 4 , respectively) was much lower than the theoretical CF (10.5) at the size range of 400–600 nm. Unfortunately the bypass period was rather short and the Q-AMS size distribution data was too noisy to be compared with the size distributions from the HR-AMS during the bypass.

However, in Table 3 we present the ratio of Q-AMS to HR-AMS mass loadings (without size distribution information) for the chemical species during the bypass period. The mass concentrations from the Q-AMS and HR-AMS in bypass agreed for sulfate and nitrate while ammonium had larger concentrations from the Q-AMS in bypass (for ammonium see comment (8) for Referee #1). In terms of organics, the mass loadings measured by the Q-AMS were smaller than those from the HR-AMS in bypass (ratio=0.7). This suggests that the low CF for organics can be partly due to the fact that the two instruments did not agree well for organics even when the Q-AMS was bypassing the ADIc. To investigate this difference, the mass spectra of organics from the Q-AMS with the ADIc and in bypass was compared to the mass spectra from the HR-AMS (in bypass) in the unit mass resolution mode (see Figure below). It is clear that m/z 44 agrees pretty well for the two instruments but the HR-AMS has more signal at most m/z 's, especially at higher m/z 's. It's possible that there was more fragmentation in the Q-AMS, but it's also possible that there was always road paving aerosol in the air and the lens cutoff affected the mass spectra even during bypass.

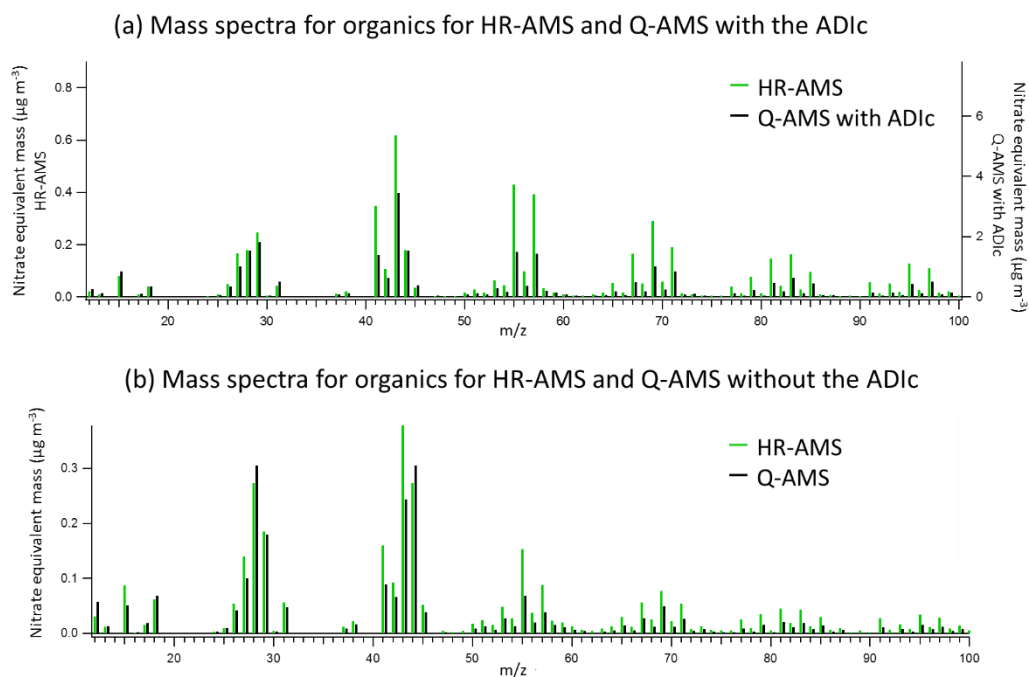


Fig. R1. Mass spectra for organics measured with the Q-AMS with the ADIc and HR-AMS in bypass (without the ADIc) (a), and the Q-AMS and HR-AMS without the ADIc (b).

Nevertheless, it can't be ruled out totally, that the concentration process was less effective for hydrocarbon-like organics than for e.g. sulfate during the field test at ARI. However, during the measurements in Helsinki, just the opposite was found. At SMEAR III hydrocarbon-like organics had higher CF than highly oxygenated organics (Fig. 4).

We added to manuscript: “Besides the lens cut-off, it is possible that the CF was smaller for hydrocarbon-like organics than for oxygenated organics during the measurements at ARI. However, that is just the opposite of what was found at SMEAR III in Helsinki where hydrocarbon-like fragment ions had higher CF than highly oxygenated fragment ions (Fig. 4).”

We added two sentences about the agreement between the two instruments during bypass:

“Average values of CF are presented in Table 3, along with the ratio of the mass loadings during bypass periods.” in the first paragraph of Section 3.2.3 and “The agreement between the two instruments during bypass periods was excellent for nitrate and sulfate (Table 3).” in the second paragraph.

Figure S5a has been changed because it contained incorrect data.

Also, “the average mass loadings” have been removed from the caption for Table 3 because the mass loadings were not presented in Table 3.

1 Laboratory and field evaluation of the Aerosol Dynamics Inc. concentrator (ADIC)
2 for aerosol mass spectrometry

3

4 Sanna Saarikoski¹, Leah R. Williams², Steven R. Spielman³, Gregory S. Lewis³, Arantzazu
5 Eiguren-Fernandez³, Minna Aurela¹, Susanne V. Hering³, Kimmo Teinilä¹, Philip Croteau², John
6 T. Jayne², Thorsten Hohaus^{2,+}, Douglas R. Worsnop², Hilkka Timonen¹

7

8 ¹ Atmospheric Composition Research, Finnish Meteorological Institute, Helsinki, Finland

9 ² Center for Aerosol and Cloud Chemistry, Aerodyne Research, Inc., Billerica, MA, USA

10 ³ Aerosol Dynamics Inc., Berkeley, CA, USA

11 ⁺ Now at Institute of Energy and Climate Research, IEK-8: Troposphere, Forschungszentrum
12 Juelich GmbH, Juelich, Germany

13

14 **Abstract**

15 An air-to-air ultrafine particle concentrator (Aerosol Dynamics Inc. concentrator; ADIc) has been
16 designed to enhance on-line chemical characterization of ambient aerosols by aerosol mass
17 spectrometry. The ADIc employs a three-stage, moderated water-based condensation growth tube
18 coupled to an aerodynamic focusing nozzle to concentrate ultrafine particles into a portion of the
19 flow. The system can be configured to sample between 1.0–1.7 L min⁻¹ with an output concentrated
20 flow between 0.08–0.12 L min⁻¹, resulting in a theoretical concentration factor (sample flow/output
21 flow) ranging from 8 to 21. Laboratory tests with monodisperse particles show that the ADIc is
22 effective for particles as small as 10 nm. Laboratory experiments conducted with the Aerosol Mass
23 Spectrometer (AMS) showed no shift in the particle size after the ADIc, as measured by the AMS
24 particle time-of-flight. The ADIc-AMS system was operated unattended over a one-month period
25 near Boston, Massachusetts. Comparison to a parallel AMS without the concentrator showed
26 concentration factors of 9.7 ± 0.15 and 9.1 ± 0.1 for sulfate and nitrate, respectively, when operated
27 with a theoretical concentration factor of 10.5 ± 0.3 . The concentration factor of organics was
28 lower, possibly due to the presence of large particles from nearby road-paving operations, and a
29 difference in aerodynamic lens cutoff between the two AMS instruments. Another field
30 deployment was carried out in Helsinki, Finland. Two ~10-day measurement periods showed good
31 correlation for the concentrations of organics, sulfate, nitrate and ammonium measured with an
32 Aerosol Chemical Speciation Monitor (ACSM) after the ADIc, and a parallel AMS without the
33 concentrator. Additional experiments with an AMS alternating between the ADIc and a bypass
34 line demonstrated that the concentrator did not significantly change the size
35 distribution or the chemistry of the ambient aerosol particles.

36

37 **1 Introduction**

38 Particles in the ambient atmosphere are of concern for human health, air quality and climate change
39 (Pope and Dockery, 2006; Lelieveld et al., 2015; IPCC 2014). Measurement of the chemical
40 characteristics of particles, and the health effects associated with their inhalation, often benefit
41 from higher sample load which can be achieved by increasing sample flow rate, extending
42 sampling time or using a particle concentrator. Enrichment of particle number or mass
43 concentration is particularly important for measurements in regions where particle concentrations
44 are low, such as in Arctic or Antarctic background areas (10–1000 particles per cm⁻³, Asmi et al.,
45 2010; Tunved et al., 2006). An increase in particle mass can also benefit the measurement of trace
46 aerosol components such as metals, or improve the determination of chemically resolved size
47 distributions.

48 Several air-to-air concentrators have been designed to increase the concentration of particles with
49 respect to the suspending gas volume, and to thereby provide enhanced aerosol detection. To
50 be beneficial, the concentrator should be small, easy to maintain and capable of operating several
51 days or even weeks unattended. Even more importantly, the concentrator should provide stable
52 enrichment of particles, and maintain aerosol chemical and physical and properties such as
53 composition and size distribution. Virtual impactors are a well-known type of air-to-air particle
54 concentrators that use a low-velocity sampling probe to sample a particle flow exiting from a
55 nozzle but they are typically ineffective for the submicrometer (< 1 μm) and ultrafine (< 100 nm)
56 particle size ranges that are of most interest for atmospheric and health-related particle studies.
57 Current air-to-air concentrators for small particles couple condensational growth with traditional
58 virtual impactors, e.g., the Versatile Aerosol Concentration Enrichment System (VACES, Kim et
59 al., 2001), the miniature VACES (Geller et al., 2006; Saarikoski et al., 2014) or the Harvard
60 Ultrafine Concentrated Ambient Particle System (HUCAPS, Gupta et al., 2004). However, these
61 systems are ineffective for particles below ~30 nm in diameter. Moreover, with long
62 condensational growth times, these approaches have been shown to feature the undesirable effect
63 of changing the particle chemical composition (e.g., Saarikoski et al., 2014).

64 Here we present a new air-to-air particle concentrator, the Aerosol Dynamics Inc. concentrator
65 (ADIC), that is based on the three-stage, laminar-flow, water-based condensational growth
66 approach used in the Sequential Spot Sampler (Eiguren Fernandez et al., 2014; Pan et al., 2016),

67 and in some water condensation particle counters (CPCs, Hering et al., 2017; 2018). This system
68 is designed specifically for instruments with low sampling flow rates on the order of 0.1 L min^{-1} .
69 It offers concentration factors (CFs) of 8 to 21 for particles as small as 10 nm diameter in an output
70 flow that is noncondensing at typical room temperatures (i.e. with dew points below $16 \text{ }^\circ\text{C}$).
71 Previously, a preliminary version of this concentration approach that used a two-stage growth tube
72 was coupled to an Aerosol Time-of-Flight Mass Spectrometer (ATOFMS, Zauscher et al., 2011)
73 and showed both concentration enhancement and lack of chemical artifacts. However, this
74 preliminary system was not stable enough for long-term operation.

75 The three-stage growth column version of the ADIc described here eliminates excess water vapor
76 in the output flow and decreases the residence time for the particle in the droplet phase, with the
77 objective of minimizing chemical artifacts as well as providing long-term stability. The ADIc is a
78 smaller scaled version of the approach used in the nano-particle charger reported by Kreisberg et
79 al. (2018), for which chemical artifacts, evaluated using Thermal Desorption Chemical Ionization
80 Mass Spectrometry, were found to be mostly insignificant. The ADIc is tailored for use with an
81 aerosol mass spectrometer, such as the Aerodyne Aerosol Mass Spectrometer (AMS), [the](#)
82 [Aerodyne Aerosol Chemical Speciation Monitor \(ACSM\)](#) or [the](#) ATOFMS. In this paper, the
83 ADIc was evaluated in laboratory experiments that explored its influence on particle size and
84 chemical composition. The ADIc was also evaluated in field measurements conducted in two
85 different environments (~~urban and~~ urban background [and suburban](#)) and with different commonly
86 used types of aerosol mass spectrometers. Moreover, long term (weeks to months) unattended
87 operation of the ADIc was demonstrated.

88

89 **2 Experimental**

90 **2.1 System description of the ADIc**

91 The ADIc uses a laminar flow, water- based condensation growth tube coupled to an aerodynamic
92 focusing nozzle to provide concentration of particles from a $1\text{--}1.7 \text{ L min}^{-1}$ sample flow into a 0.08--
93 0.12 L min^{-1} concentrated output flow. This system uses a three-stage moderated aerosol
94 condensation approach (Hering et al., 2014) whereby the aerosol flow passes through a wet-walled
95 tube with three distinct temperature regions (Fig. 1). In the first stage, the conditioner has cold
96 walls and brings the flow to known conditions of cool temperature and high relative humidity

97 (RH). The second, initiator stage, has warm walls and provides the water vapor that creates the
98 supersaturation for particle activation, while the last, cool-walled moderator stage provides time
99 for particle growth while simultaneously removing water vapor from the flow. The water vapor
100 saturation level reaches a value of 1.4 in the initiator while maintaining temperatures below 30 °C
101 in the majority of the sample flow, and simultaneously providing for output flow dew points below
102 16 °C. Thus, the water vapor content of the output flow is reduced to typical ambient conditions,
103 making it easier to handle, and minimizing the amount of water reaching the detection system. The
104 wetted walls are maintained by a single wick formed from rolled membrane filter media and the
105 flow is laminar throughout the ADIc system.

106 Within the growth tube, particles with diameters above 5–10 nm are activated and grow by
107 condensation to form droplets of approximately 1.5–4 μm in diameter. The cooled, droplet-laden
108 flow passes through a 1-mm diameter nozzle wherein the droplets are aerodynamically focused
109 along the central core of the flow, much as described by Fuerstenau et al. (1994). The ADIc
110 contains an annular slit in the side wall of this nozzle, through which the majority (85–95 %) of
111 the flow (discard flow) is extracted. The remaining 5–15 % of the flow contains the droplets which
112 have been focused aerodynamically. Water evaporates from the droplets once the flow regains
113 ambient (20–25 °C) temperature to provide a concentrated aerosol flow (output flow). The system
114 is designed to minimize the time the particle is a droplet, with the objective of minimizing chemical
115 artifacts, similar to the nano-particle charging system (Kreisberg et al., 2018).

116 The exact design of the focusing and flow extraction nozzle is based on numerical modeling done
117 using the Comsol Multiphysics package. Numerical modeling results, presented in Fig. S1 for the
118 final design, show that particles smaller than 1 μm follow the gas flow trajectories and are extracted
119 through the annular slit while those above 6 μm over-focus and collide with the opposite wall.
120 However, intermediately sized particles, corresponding to a Stokes number (St) of 0.5 to 3.5, are
121 aerodynamically focused in the region near the centerline of the flow. These particles follow the
122 remaining flow, the output flow, which continues straight, thus providing a concentrated flow for
123 sampling with aerosol instrumentation. The theoretical concentration factor is determined by the
124 ratio of the sample flow rate to the output flow rate and can be varied between 8 and 21.

125 Two prototype concentrators (Prototype 1 and 2) were used in this study, both having the same
126 dimensions for the growth tube and nozzle. The conditioner, initiator and moderator are 140 mm,

127 51 mm and 102 mm long, respectively, separated by 7.5 mm thick insulator sections. In both
128 prototypes the growth tube was lined with a 9 mm-ID, ~1.5 mm-thick wick formed from rolled
129 membrane filter. For particles along the centerline of the flow, the calculated residence time from
130 the point of activation to the inlet of the focusing nozzle is 200–300 ms, depending on the point of
131 activation. Along the flow trajectory that encompasses 50% of the flow, the residence time is as
132 long as 400 ms.

133 The conditioner and moderator were cooled using Peltier heat pumps and the initiator and focusing
134 nozzle were heated resistively. All three regions used proportional-integral-derivative (PID)
135 control to maintain set-point temperatures. Distilled water was injected into the initiator stage at a
136 rate of 5 $\mu\text{L min}^{-1}$ and excess water was removed from the base of the wick carried by a small flow
137 of $\sim 0.05 \text{ L min}^{-1}$ of air into a waste bottle. Other than packaging, the only difference between the
138 prototypes was that Prototype 1 had a mass flow meter to measure the discard flow while Prototype
139 2 did not have this option. The theoretical CF for Prototype 1 was determined continuously from
140 the measured flows, while for Prototype 2 the theoretical CF was determined from the sample and
141 concentrated flow rates measured before and after each experiment. The size of the ADIc is
142 approximately 30 x 30 x 50 cm (W x D x H) and the weight is $\sim 11 \text{ kg}$.

143

144 **2.2 Evaluation in the laboratory**

145 **2.2.1 Particle number measurements at ADI**

146 The performance of the ADIc for particle counting was evaluated in the laboratory at Aerosol
147 Dynamics Inc. (ADI) using monodisperse particles generated by atomization, followed by drying
148 and charge conditioning (soft X-ray, Model 3087, TSI Inc., Shoreview, US). Particles were size
149 selected using a nano-differential mobility analyzer (DMA, Model 3085, TSI Inc., Shoreview, US)
150 for sizes between 5 nm and 60 nm and using the Aerosol Dynamics Inc. high-flow DMA
151 (Stolzenburg et al., 1998) for sizes between 20 nm and ~~4~~600 nm. Particle concentrations were
152 measured in the sample flow and in the concentrated output flow using water-based CPCs.
153 Prototype 1 was evaluated with mono-mobility ammonium sulfate (AS) particles with a pair of
154 prototype Model 3785 (TSI Inc., Shoreview, US) water-based CPCs and a Model 3783 CPC (TSI
155 Inc., Shoreview, US) to simultaneously measure particle concentrations in the sample flow, in the

156 discard flow, and in the concentrated output flow, respectively. The sample flow was fixed at 1.0
157 L min⁻¹; and the output flow was 0.12 L min⁻¹ (theoretical CF = 8.3). The operating temperatures
158 for conditioner (Tcon), initiator (Tini), moderator (Tmod) and focusing nozzle (Tnoz) were 5, 26,
159 10 and 30 °C, respectively (see Table 1).

160 Similar evaluation experiments were carried out on Prototype 2 but its operation was tested under
161 two flow regimes. First, experiments were done at 1.0 L min⁻¹ sample flow and 0.11 L min⁻¹ output
162 flow (theoretical CF = 9.1), with similar operating temperatures to Prototype 1. To test higher CFs,
163 experiments were also done at a sample flow rate of 1.5 L min⁻¹ and an output flow of 0.11
164 L min⁻¹ for a theoretical CF of 13.6. The growth tube is sized for low-flow operation, such that the
165 centerline supersaturation reaches its maximum at the end of the warm initiator section. At the
166 higher flow rate, the residence time is shorter, and thus for the same operating temperatures the
167 peak supersaturation is lower. To compensate, the initiator was operated at a warmer wall
168 temperature, thereby providing a similar value for the calculated peak super-saturation. The
169 operating temperatures for the higher flow rate were Tcon = 6 °C, Tini = 31 °C, Tmod = 8 °C, and
170 Tnoz = 35 °C (Table 1).

171 In addition to laboratory generated AS particles, both prototypes were tested with laboratory air
172 using a pair of water-based CPCs, one sampling upstream of the ADIc and one sampling
173 downstream.

174

175 2.2.2 Particle chemistry at ARI and FMI

176 The performance of the ADIc in terms of particle chemistry was evaluated at Aerodyne Research,
177 Inc. (ARI) and at the Finnish Meteorological Institute (FMI). Laboratory experiments were carried
178 out by using particles generated with a constant output atomizer (Model 3076, TSI Inc., Shoreview,
179 US) from AS or ammonium nitrate (AN) in deionized water, or from dioctyl sebacate (DOS) in 2-
180 propanol. Generated particles were dried with a silica gel dryer and the desired monodisperse
181 particle size fraction was selected using a DMA (Model 3080, TSI Inc., Shoreview, US). A valve
182 system was used to alternate between passing the particles through the ADIc and bypassing it.
183 Temperature and flow settings used in the ADIc during the ARI and FMI experiments are given
184 in Table 1.

185 Particle size and chemical composition were measured with several different versions of the AMS,
186 including a high-resolution time-of-flight aerosol mass spectrometer (HR-AMS, Aerodyne
187 Research Inc., Billerica, US; DeCarlo et al., 2006), a soot-particle aerosol mass spectrometer (SP-
188 AMS, Aerodyne Research Inc., Billerica, US; Onasch et al., 2012), a quadrupole aerosol mass
189 spectrometer (Q-AMS, Aerodyne Research Inc., Billerica, US; Canagaratna et al., 2007) and a
190 quadrupole aerosol chemical speciation monitor (ACSM, Aerodyne Research Inc., Billerica, US;
191 Ng et al., 2011). These instruments all operate on the same principle. Aerosol particles are sampled
192 through an aerodynamic lens, forming a narrow particle beam that is transmitted into the detection
193 chamber where the non-refractory species are flash vaporized upon impact on a hot surface (600
194 °C). The particle vapor is ionized using electron impact ionization (70 eV) and detected by the
195 mass spectrometer. Particle size (particle time of flight, (PToF) data) is determined from particle
196 flight time in the vacuum chamber after passing through a chopper. The typical size range of
197 particles detected with an AMS is 70 nm to 700 nm (Liu et al., 2007). In addition to the thermal
198 vaporizer, the SP-AMS incorporates an intracavity Nd-YAG (1064 nm) laser that enables the
199 detection of refractory black carbon (rBC) and metal containing particles (Onasch et al.,
200 2012; Carbone et al., 2015). The ACSM does not include particle size measurement capability.

201 HR- and SP-AMS data was analyzed with the Squirrel (v1.57H)/Pika (v1.16H) and Squirrel
202 (v1.60P)/Pika (v1.20P) analysis package, respectively. Additionally, high resolution (HR) size
203 distribution data from the SP-AMS was analyzed with the Squirrel (v1.62A)/Pika (v1.22A)
204 package. Both the HR-AMS and SP-AMS instruments were equipped with a multiplex chopper
205 (efficient Particle Time of Flight, ePToF, chopper) with 50% particle throughput. ~~and~~ The
206 measured size distributions were normalized to the mass concentrations measured in the mass
207 spectrum mode. Q-AMS data was analyzed with AMS Analysis Toolkit 1.43. ACSM data was
208 analyzed with ACSM Local (v1.6.1.1). All of the analysis software runs in the Igor 6
209 (WaveMetrics, Inc.) programming environment. The three AMS instruments and the ACSM were
210 calibrated for ionization efficiency (IE) of nitrate and relative ionization efficiency (RIE) of both
211 ammonium and sulfate, using size selected single component particles of AN or AS
212 (Budisulistiorini et al., 2014).

213

214 2.3 Field testing

215 The ADIc was tested for ambient aerosol at two different locations. At ARI, particles were sampled
216 from a roof top sampling station on the ARI building at 45 Manning St., Billerica, MA (42.53, -
217 71.27, 60 m a.s.l.), located in a suburban office park about 30 km NW of Boston, MA and located
218 about 60 m NE of ~~6-lane major~~ freeway. Ambient air was sampled at 3 L min⁻¹ through a 2.5 μm
219 cut cyclone and split between two paths. The first path went to an HR-AMS and a CPC (Model
220 3776, TSI Inc., Shoreview, US). The second path went to the ADIc followed by a Q-AMS and a
221 CPC (Model mCPC, Brechtel, Hayward, US). Two valves allowed the ambient air to bypass the
222 ADIc and directly enter the Q-AMS. Both AMSs recorded data at 2-minute time resolution.
223 Ambient sampling was conducted from 1 to 26 August 2014. The default collection efficiency
224 (CE) of 0.5 for ambient particles was applied to data from both AMS instruments. Local ambient
225 temperature was downloaded from Weather Underground for station KMABILLE10 and ambient
226 RH data was downloaded from NOAA for Hanscom.

227 The second ambient sampling location was at an urban background station (SMEAR_III; Station
228 for Measuring Ecosystem-Atmosphere Relationships, 60.20, 24.95, 30 m a.s.l., described by Järvi
229 et al., 2009) located at the Kumpula campus near the FMI building, about 5 km NE of the Helsinki
230 city center, Finland. The station is surrounded by office buildings on one side and a small forest
231 and botanical garden on the other side. Ambient particles were sampled through a 2.5 μm cyclone
232 with a flow rate of 3 L min⁻¹. Sample flow was split into two sampling lines; the first line went to
233 the SP-AMS (with an additional bypass flow of 1.3–2 L min⁻¹) and the second line to the ADIc
234 followed by an ACSM. The ACSM data was averaged approximately to 10-minute time resolution
235 (10 times open + close, m/z range: 10–150, scan rate 200 ms/amu) and the SP-AMS measured
236 with a time resolution of 1.5 minutes. Two sample flow regimes were tested with the ACSM+ADIc
237 system; the sample flow was set to either 1.7 L min⁻¹ or 1.0 L min⁻¹ while the output flow of the
238 ADIc was determined by the ACSM inlet flow of 0.08 L min⁻¹, giving a theoretical CF of 21.3 and
239 12.5 for high and low sample flow, respectively. Additionally, in a separate set of experiments, the
240 ADIc was installed upstream of the SP-AMS in order to investigate the influence of the ADIc on
241 high resolution mass spectra and size distributions. Those tests were carried out in the high flow
242 regime (theoretical CF of 21.3) in order to maximize the increase in HR organic and rBC mass
243 spectral and PToF signals with the ADIc. The SP-AMS measurements were conducted by
244 switching the laser on/~~and~~ off every 1.5 minutes. Laser off data was utilized when the SP-AMS
245 was compared with the ACSM+ADIc and laser on data was used for the period when the ADIc

246 was installed in front of the SP-AMS. The default CE of 0.5 for ambient particles was applied to
247 both ACSM and SP-AMS data. An RH sensor was installed in the ACSM line after the ADIc.
248 Ambient meteorological parameters were recorded at the Kumpula Weather station. Field
249 measurements at SMEAR III were conducted between 13 July to 22 October 2018, with sampling
250 on about 27 different days. Temperature settings of the ADIc during the field campaigns at ARI
251 and FMI are given in Table 1. [Instrumental setups used in the laboratory and field tests at ADI,](#)
252 [ARI and FMI are shown in Fig. S2.](#)

253

254 **3 Results and discussion**

255 **3.1 Laboratory evaluation**

256 **3.1.1 Concentration factor**

257 Figure 2 shows laboratory results for monodisperse AS particles for two flow regimes. The
258 measured concentration factor, defined as the ratio of particle number concentration in the output
259 flow of the ADIc to that in the sample flow, is plotted as a function of particle mobility diameter.
260 Data for the lower flow regime is from Prototype 1, which was subsequently tested at ARI for
261 aerosol chemical species. For the lower flow, the average measured CF was 7.7 ± 0.3 for the
262 particles larger than 15 nm, compared to a theoretical CF of 8.3. Data shown for the higher flow
263 regime was obtained with Prototype 2, which was later tested at FMI for particle chemistry and
264 size distributions. For the higher flow, the measured CF was 11.9 ± 0.2 , compared to a theoretical
265 CF of 13.6, for 50–305 nm particles. When operated in the lower flow regime, Prototype 2 data is
266 similar to that for Prototype 1, with a measured CF of 7.0 ± 0.5 (data not shown). The influence of
267 ADIc on particle size was investigated in more detail with aerosol mass spectrometers (Sect.
268 3.1.2.).

269 The ratio of measured to theoretical CF was ~ 0.9 (see Table 2), suggesting that 90 % of the
270 particles in the sample flow were focused into the output concentrated flow. In the experiments
271 conducted on Prototype 1, the particle concentration was also measured in the discard flow, and it
272 accounted for 9 ± 2 % of the sampled particle concentration at sizes above 20 nm, on average. The
273 fraction of particles in the discard flow showed a small, but systematic, dependence on particle
274 size with the fraction decreasing from 12 % at 18 nm to 6 % at 600 nm. The unaccounted [for](#)

275 particles (2 % on average) were presumably lost in the transport lines or in the focusing nozzle
276 itself.

277 To evaluate the stability of the ADIc, both prototypes were operated for several days while
278 sampling laboratory air. Particle number concentrations were measured in the sample flow and in
279 the output flow. Particle concentration varied between 900 and 15000 # cm⁻³. For the lower flow
280 regime data (Fig. S32a-b), the ~~measured average CF, calculated as the ratio of the number~~
281 ~~concentration in the output flow to that in the sample flow,~~ was ~~of~~ $5.765.87 \pm 0.404$ with ~~at~~
282 theoretical CF of 7.5. Linear regression of that data yielded a correlation coefficient (R²) of 0.984.
283 In the higher flow regime (Fig. S32c-d), the measured CF was 99.0 ± 0.7107 , with a
284 theoretical CF of 13.6. For that data the correlation coefficient (R²) was 0.940. It is important to
285 note that particle concentrations were measured using CPCs with a 5 nm activation threshold while
286 the ADIc threshold is closer to 10 nm. Thus, particles below 10 nm in the ambient size distribution
287 would not be concentrated, leading to a lower measured CF and a lower ratio of
288 measured/theoretical CF than in Table 2. In addition, changes in the ambient size distribution can
289 lead to some variability in the measured CF. Importantly, no systematic change was observed
290 throughout the experiments.

291

292 3.1.2 Chemical composition and particle size

293 The dependence of CF on particle chemical composition was evaluated in the laboratory with size-
294 selected 300 nm AS and AN particles ~~and a subsequent analysis of concentrated aerosol by~~
295 ~~sampling with the~~ ~~HRQ-AMS~~ ~~with and without the ADIc in front.~~ The theoretical and the
296 measured CF for ammonium and sulfate from AS and for ammonium and nitrate from AN are
297 given in Table 2. Compared to ~~the~~ CF obtained for particle number concentration, the ratio of
298 measured to theoretical CF was the same for AS while for AN the measured CF was slightly closer
299 to the theoretical CF.

300 The influence of the ADIc on particle size was investigated by using monodisperse AS, AN and
301 DOS particles in the size range of 30 to 340 nm (mobility diameter). Size and chemical
302 composition of particles with and without the ADIc were analyzed by an SP-AMS. Measurements
303 were carried out in the high flow regime (theoretical CF of 21.3). Figure 3 shows the vacuum

304 aerodynamic diameter (d_{va}) for sulfate (from AS), nitrate (from AN) and organics (from DOS) as
305 measured for concentrated versus unconcentrated aerosol. The regression slope was 1.02, the
306 intercept was -2.51, and the correlation coefficient (R^2) was 0.999 showing that the particle
307 diameter was not changed by passing through the ADIc for any of the measured particle sizes or
308 chemical species.

310 3.2 Field Evaluation

311 3.2.1 Ambient organics and rBC

312 The performance of the ADIc for ambient aerosol was examined at two locations; at a roof top
313 sampling station on the ARI building and at SMEAR III in Helsinki. In order to investigate the
314 impact of the ADIc on aerosol organic and rBC chemistry, the SP-AMS was installed behind the
315 ADIc at SMEAR III and alternated every 30 minutes between measuring ~~alternately from~~ the
316 output flow of the ADIc and a bypass line with 30 minutes time periods. Measurements were
317 performed on 11 different days in June, July and August 2018 with a total sampling time of ~7
318 hours behind the ADIc and ~7 hours in bypass. Average high-resolution mass spectra for organics
319 and rBC with and without the ADIc are presented in Fig. 4. In general, organics at SMEAR III
320 were highly oxygenated with large oxygen to carbon ratio (O:C) and large organic carbon to
321 organic matter ratio (OC:OM). The elemental composition of organics did not change noticeably
322 when the sample was passed through the ADIc.

323 The correlation between the mass spectral ions with and without the ADIc for each fragment family
324 are presented in Fig. 4 c-f. The correlation was uniformly high ($R^2 > 0.987$) and the slope
325 describing the measured CF was ~~on average smaller than theoretical CF (21.3) for all the families~~
326 ~~except the C_x (rBC) family 19.2 ± 3.2 . The slope was smallest for the most oxygenated fragment~~
327 ~~family $C_xH_yO_z$, $z > 1$ and largest for C_x (rBC) and was smaller than theoretical CF (21.3) for all~~
328 ~~families except the C_x family.~~ Smaller measured than theoretical CF is in agreement with the
329 results obtained in the laboratory tests (see Table 2) while the reason for a larger measured than
330 theoretical CF for C_x is still unclear. One possible explanation is that the ADIc altered the shape
331 of the rBC-containing particles. The effect of the condensation/evaporation process on particle
332 shape was not explored in this study; however, others have found changes in the shape of

333 aggregates. In a study using a condensation system similar to that employed here, Ma et al (2013)
334 reported collapse of the aggregate structure of laboratory-generated soot in the evaporation
335 process. For a hygroscopic salt (ammonium sulfate), Kreisberg et al (2018) observed that the
336 condensation process could produce an increase in particle size unless the sample was heated to at
337 least temporarily to reduce the relative humidity below the effervescence point. Regarding the SP-
338 AMS, the morphology of the particles had been demonstrated to affect the collection efficiency of
339 the SP-AMS since it affects the overlap of the particle beam and the laser beam (Willis et al.,
340 2014).

341 Overall, based on these tests, it can be concluded that passing through the ADIc does not
342 significantly change the fragmentation or the elemental composition of organics or rBC in the
343 ambient particles. However, due to the larger CF for rBC than for organics the mass fraction of
344 rBC in ambient particles increased slightly with the ADIc (Fig. S4).

346 **3.2.2 Mass size distributions**

347 The SP-AMS data with and without the ADIc was also used to investigate the impact of the ADIc
348 on particle mass size distributions. Figure 5 compares the mass size distribution for organics,
349 sulfate, nitrate and ammonium sampling through the ADIc and sampling from the bypass line. The
350 PToF data was collected and analyzed in unit mass resolution (UMR) mode. Figure 5 demonstrates
351 that the size distribution of ambient aerosol particles was not affected by passing through the ADIc.
352 In addition, Fig. 5d shows significant improvement in signal to noise for ammonium when
353 concentrating the sample flow.

354 Additional SP-AMS size distribution data was collected and analyzed in HR mode on one day with
355 a total sampling time of 70 minutes in bypass and 70 minutes through the ADIc. HR size
356 distributions are shown in Fig. 6 for major chemical species and for several specific fragment ions.
357 The much higher signal to noise in the concentrated PToF traces gives better chemical resolution
358 of the size distribution. The bimodal size distribution for organics is clear in the ADIc data in Fig.
359 6a with hydrocarbon-like fragments (e.g., C₃H₇ and C₄H₉ in Fig. 6h and 6k) contributing to the
360 mode at $d_{va} = 160$ nm and more oxygenated fragments (e.g., C₂H₃O, CO₂, C₂H₄O₂ and C₃H₅O in
361 Fig. 6g, 6i, 6j and 6l) contributing to the mode at $d_{va} = 400$ nm. In addition, the higher signal to

362 noise in the concentrated sample enables PToF measurement for very small signals such as
363 chloride (Fig. 6e) or CO₂ (Fig. 6i) and improves the PToF measurement for smaller signals such
364 as rBC (Fig. 6f).

365

366 3.2.3 Long-term Stability

367 The long-term operation of the ADIc was tested at ARI where it ran for more than three weeks
368 without user maintenance or intervention. The measured CFs from comparing the Q-AMS mass
369 loading to the HR-AMS mass loading are presented in Fig. 7. With the average values of CF are
370 presented in Table 3, along with the ratio of the mass loadings during bypass periods. The
371 theoretical CF was calculated from the ADIc discard flow rate and the Q-AMS inlet flow rate
372 (equal to ADIc outlet flow) as theoretical CF = (discard flow + Q-AMS inlet flow)/Q-AMS inlet
373 flow. Discard and Q-AMS flows were logged in real-time. The slight variation in theoretical CF
374 was due to variations in the Q-AMS inlet flow rate, not variations in the discard flow. The gap in
375 the data between 21 and 23 August 2014 was due to an issue with the HR-AMS, not with the ADIc.

376 The measured CFs for nitrate and sulfate were 85 to 90 % of theoretical CFs, consistent with the
377 laboratory measurements presented in Table 2. The agreement between the two instruments during
378 bypass periods was excellent for nitrate and sulfate (Table 3). The measured CF for ammonium
379 was higher than the theoretical value which may indicate that the aqueous droplets in the ADIc
380 initiator and moderator stages absorbed gas-phase ammonia that remained in the particles after
381 drying. This effect has been observed for acidic particles in the miniature VACES (Saarikoski et
382 al., 2014). The ambient aerosol in this study was possibly slightly acidic with an average ratio of
383 measured to predicted ammonia of 0.9 ± 0.15 in the HR-AMS data. Another possibility is that the
384 RIE for ammonium was incorrect for one or both of the instruments, even though it was measured
385 before and after the ambient sampling period with pure AN particles. The CF during bypass periods
386 was 1.3 ± 0.4 (Table 3) indicating that the two instruments did not agree well for ammonium even
387 when the Q-AMS was bypassing the ADIc. However, the ammonium mass loading was low (<0.4
388 $\mu\text{g m}^{-3}$) and often close to the detection limit for the Q-AMS during the bypass periods, leading to
389 a large uncertainty in the bypass CF, three times during the experiment. This is supported by the
390 fact that the measured CF was greater than one during periods when the Q-AMS was bypassing
391 the ADIc (Table 3).

392 The measured concentration factor (6.1 ± 0.8) for organics was much lower than the theoretical
393 value (10.5 ± 0.3). This ~~was~~ could be partly caused by a difference in the cutoff of the aerodynamic
394 lenses in the two AMS instruments. During this time period, organics were dominated by
395 emissions from road paving activities which generate large, hydrocarbon-like particles. Figure ~~S3~~
396 S5 shows the size distributions for organics, mass-to-charge ratio (m/z) 44, and m/z 57 for the HR-
397 AMS and the Q-AMS+ADIC. ~~It is clear that~~ the size distributions for organics and m/z 57 from
398 the Q-AMS were missing mass above $d_{va} \sim 700$ nm that was measured by the HR-AMS, leading
399 to a lower measured CF for organics. The m/z 44 size distributions, representative of accumulation
400 mode aerosol particles, were similar in the two instruments because the ~~mass of m/z 44 size~~
401 distribution of these particles was below the lens cutoff. The measured CF for m/z 44 in Fig. S3b
402 was 9.2 while the measured CF for m/z 57 in Fig. S3c was only 3.9. The measured CF for organics
403 also showed a larger diurnal variation than the measured CFs for the other species (Fig. 7), likely
404 because road paving activities took place at night leading to a lower measured CF at night-time.
405 Besides the lens cut-off, it is possible that the CF was smaller for hydrocarbon-like organics than
406 for oxygenated organics during the measurements at ARI. However, that is just the opposite of
407 what was found at SMEAR III in Helsinki where hydrocarbon-like- ~~organics~~ fragment ions had
408 higher CF than highly oxygenated- ~~organics~~ fragment ions (Fig. 4).

409

410 3.2.4 Concentrating under high and low flow regimes

411 The performance of the ADIC with ambient aerosol was also tested systematically under two flow
412 regimes. Although the growth tube in the ADIC is sized for low-flow operation, in some cases it
413 can be beneficial to operate the ADIC with the largest possible CF, for example, when very small
414 signals (e.g., metals, PToF) are of interest, or the ambient concentrations are extremely low. High
415 (1.7 L min^{-1}) and low (1.0 L min^{-1}) sample flows, resulting in theoretical CFs of 21.3 and 12.5,
416 respectively, were investigated at SMEAR III with the ADIC installed in front of an ACSM while
417 the SP-AMS was sampling from the bypass line. The data from the ACSM+ADIC was corrected
418 for the CF by dividing the concentrations by $0.9 \times$ theoretical CF since the laboratory tests and the
419 field campaign at ARI suggest that the measured CF is likely to be 90 % of the theoretical CF.

420 The time series of all chemical species measured with the ACSM+ADIC and SP-AMS track each
421 other well and the average mass loadings agreed within 20–30 % (Fig. 8), within the estimated

422 uncertainty of 34–38 % for AMS measurements (Bahreini et al., 2009). In the high flow regime,
423 the corrected ACSM+ADIC mass loadings were systematically higher for organics, sulfate and
424 ammonium compared to the SP-AMS. This might be caused by the lack of simultaneous
425 measurement of the sample flow rate, so that any error in the sample flow rate before/after the
426 experiment could propagate into the theoretical CF and thus into the correction factor. For nitrate,
427 the corrected ACSM+ADIC mass loading varied above the SP-AMS during the afternoon and
428 below during the night. Under low flow conditions, there was a time period of about 12 hours on
429 18 and 19 September when the corrected ACSM+ADIC mass loadings for nitrate and chloride were
430 much lower than corresponding mass loadings from the SP-AMS. During this period, the aerosol
431 particles were also not neutralized (i.e., measured ammonium was lower than ammonium predicted
432 from the measured anions). Based on the ratio of m/z 46 to m/z 30, nitrate was in the form of
433 inorganic nitrate (e.g., NH_4NO_3) rather than organic nitrates. The reason for the lower
434 concentrations of nitrate and chloride with the ACSM+ADIC during this 12 hour period is not
435 clear.

436 The relative humidity was measured after the ADIC near the Q-ACSM inlet. RH was relatively
437 constant at 63 ± 6 %, consistent with a dewpoint of 16 °C at the outlet of the ADIC and a room
438 temperature of about 25 °C. This was somewhat higher than the recommended operating RH of
439 20–40 % for AMS/ACSM instruments, but not high enough to cause an increase in the collection
440 efficiency (Middlebrook et al., 2012). However, using a dryer in between the ADIC and the
441 AMS/ACSM would reduce any potential uncertainty due to RH affecting CE.

442 In terms of Q-ACSM measurement, a particularly important improvement in signal to noise with
443 the ADIC was achieved. Figs. 9a and 9b show 30-minute time resolution data collected with the
444 Q-ACSM without the ADIC, and Figs. 9b and 9d display 10-minute time resolution data collected
445 with the Q-ACSM+ADIC for ammonium and m/z 60, a tracer m/z for biomass burning. Compared
446 to the SP-AMS data averaged to the same time resolution, it is evident that the signal to noise for
447 the concentrated Q-ACSM data is similar to the SP-AMS. As a consequence, use of the ADIC with
448 the ACSM will improve determination of ammonium and thus provide better estimates of particle
449 neutralization and CE for ambient aerosol. In addition, better signal to noise for tracer m/z 's will
450 improve source apportionment with statistical methods such as positive matrix factorization
451 (PMF).

452

453 **4 Conclusions**

454 The ADIc is tailored for the low ($\sim 0.08 \text{ L min}^{-1}$) inlet flow of aerosol mass spectrometers such as
455 the AMS and ACSM and provides a factor of 8–21 enrichment in the concentration of particles.
456 This concentration factor depends primarily on the ratio between the sample flow and the output
457 flow, and is found to be independent of particle size above about 10 nm. The system is relatively
458 small, and easily interfaced with the AMS.

459 Particle chemical composition and particle size measured with an SP-AMS were not affected by
460 the condensational growth and evaporation process in the ADIc. Moreover, the ADIc ran
461 unattended for a period of almost one month at a field site. Measured concentration factors for
462 ambient aerosol particles in two different locations showed some variation that is not fully
463 understood. However, the ADIc provides improved detection of low signals that outweighs a slight
464 increase in uncertainty in the mass loadings. Improved detection limits will be important especially
465 in remote areas where particle concentrations are low, and for measuring size distributions that
466 typically need longer averaging periods. Additionally, use of the ADIc will be important for
467 improving source apportionment with Q-ACSM data by gaining better time-resolution and/or
468 signal to noise ratio.

469

470 *Data availability.* Data presented in this article is available upon request.

471

472 *Supplement.* The supplement related to this article is available online

473

474 *Competing interests.* Aerosol Dynamics Inc. holds a patent on the particle focusing technology.

475

476 *Author contributions.* SS, HT, SVH, AEF and LRW designed the experiments. MA, KT, LRW,
477 PC, TH, AEF, SRS, and GSL conducted measurements in laboratory and field. Data analysis and
478 interpretation of the measurement data was done by SS, LRW, AEF and SVH. Working

479 environment and financial support was provided by HT at FMI, JTJ and DRW at Aerodyne and
480 SVH at Aerosol Dynamics. SS, LRW and SVH prepared the manuscript with contributions from
481 all co-authors.

482
483 *Acknowledgements.* Funding is gratefully acknowledged from the US Department of Energy,
484 Small Business Research Program (grant # DESC0004698), the Cityzer (Business Finland project
485 Dnro:3021/31/2015), TAQIITA (Business Finland project Dnro:2634/31/2015) and the Launching
486 Regional Innovations and Experimentations Funds (AIKO), governed by the Helsinki Regional
487 Council (project HAQT, AIKO014).

488
489

490 **References**

491 Asmi, E., Frey, A., Virkkula, A., Ehn, M., Manninen, H. E., Timonen, H., Tolonen-Kivimäki, O.,
492 Aurela, M., Hillamo, R., and Kulmala, M.: Hygroscopicity and chemical composition of Antarctic
493 sub-micrometre aerosol particles and observations of new particle formation, *Atmos. Chem. Phys.*,
494 10, 4253–4271, 2010.

495 Bahreini, R., Ervens, B., Middlebrook, A., Warneke, C., De Gouw, J., DeCarlo, P., Jimenez, J.,
496 Brock, C., Neuman, J., Ryerson, T., Stark, H., Atlas, E., Brioude, J., Fried, A., Holloway, J. S.,
497 Peischl, J., Richter, D., Walega, J., Weibring, P., Wollny, A. G., and Fehsenfeld, F. C.: Organic
498 aerosol formation in urban and industrial plumes near Houston and Dallas, Texas, *J. Geophys. Res.*
499 114, <https://doi.org/10.1029/2008JD011493>, 2009.

500 Budisulistiorini, S., Canagaratna, M., Croteau, P., Baumann, K., Edgerton, E., Kollman, M., Ng,
501 N., Verma, V., Shaw, S., and Knipping, E.: Intercomparison of an Aerosol Chemical Speciation
502 Monitor (ACSM) with ambient fine aerosol measurements in downtown Atlanta, Georgia, *Atmos.*
503 *Meas. Tech.*, 7, 1929–1941, 2014.

504 Canagaratna, M. R., Jayne, J. T., Jimenez, J. L., Allan, J. D., Alfarra, M. R., Zhang, Q., Onasch,
505 T. B., Drewnick, F., Coe, H., Middlebrook, A., Delia, A., Williams, L. R., Trimborn, A. M.,
506 Northway, M. J., DeCarlo, P. F., Kolb, C. E., Davidovits, P., and Worsnop, D. R.: Chemical and
507 Microphysical Characterization of Ambient Aerosols with the Aerodyne Aerosol Mass
508 Spectrometer, *Mass Spectrom. Rev.*, 26, 185–222, 2007.

509 Carbone, S., Onasch, T., Saarikoski, S., Timonen, H., Saarnio, K., Sueper, D., Rönkkö, T., Pirjola,
510 L., Häyriäinen, A., Worsnop, D., and Hillamo, R.: Characterization of trace metals on soot particles
511 with the SP-AMS: detection and quantification, *Atmos. Meas. Tech.*, 8, 4803–4815, 2015.

512 DeCarlo, P. F., Kimmel, J. R., Trimborn, A., Northway, M. J., Jayne, J. T., Aiken, A. C., Gonin,
513 M., Fuhrer, K., Horvath, T., Docherty, K. S., Worsnop, D. R., and Jimenez, J. L.: Field-deployable,
514 high-resolution, time-of-flight aerosol mass spectrometer, *Anal. Chem.*, 78, 8281–8289,
515 doi:10.1021/ac061249n, 2006.

516 Eiguren Fernandez, A., Lewis, G. S., and Hering, S. V.: Design and Laboratory Evaluation of a
517 Sequential Spot Sampler for Time-Resolved Measurement of Airborne Particle Composition,
518 *Aerosol Sci. Technol.*, 48, 655–663, 2014.

519 Fuerstenau, S., Gomez, A., and J. Fernandez de la Mora, J.: Visualization of aerodynamically
520 focused subsonic aerosol jets, *J. Aerosol Sci.*, 25, 165–173, 1994.

521

522 Geller, G. D., Biswas, S., Fine, P. M., and Sioutas, C.: A new compact aerosol concentrator for
523 use in conjunction with low flow-rate continuous aerosol instrumentation, *J. Aerosol Sci.*, 36,
524 1006–1022, 2005.

525 Gupta, T., Demokritou, P., and Koutrakis, P.: Development and Performance Evaluation of a High
526 Volume Ultrafine Particle Concentrator for Inhalation Toxicological Studies, *Inhal. Toxicol.*, 16,
527 1–12, 2004.

528 Hering, S. V., Spielman, S. R., and Lewis, G. S.: Moderated, water-based, condensational particle
529 growth in a laminar flow, *Aerosol Sci. Technol.*, 48, 401–408, 2014.

530 Hering, S. V., Lewis, G. S., Spielman, S. R., and Eiguren-Fernandez, A.: A MAGIC Concept for
531 Self-Sustained, Water based, Ultrafine Particle Counting, *Aerosol Sci. Technol.*, 53, 63-72, 2018.

532 IPCC: Climate Change Synthesis Report. Contribution of Working Groups I, II and III to the Fifth
533 Assessment Report of the Intergovernmental Panel on Climate Change [Core Writing Team, R.K.
534 Pachauri and L.A. Meyer (eds.)]. IPCC, Geneva, Switzerland, 151 pp. 2014. 2014.

535 Jung, H., Arellanes, C., Zhao, Y., Paulson, S., Anastasio, C., and Wexler, A.: Impact of the
536 Versatile Aerosol Concentration Enrichment System (VACES) on Gas Phase Species, *Aerosol
537 Sci. Technol.*, 44, 1113–1121, 2010.

538 Järvi, L., Hannuniemi, H., Hussein, T., Junninen, H., Aalto, P. P., Hillamo, R., Mäkelä, T.,
539 Keronen, P., Siivola, E., Vesala, T., and Kulmala, M.: The urban measurement station SMEAR
540 III: Continuous monitoring of air pollution and surface-atmosphere interactions in Helsinki,
541 Finland, *Boreal Environ Res*, 14, 86–109, 2009.

542 Khlystov, A., Zhang, Q., Jimenez, J. L., Stanier, C., Pandis, S. N., Canagaratna, M. R., Fine, P.,
543 Misra, C., and Sioutas, C.: In situ concentration of semi-volatile aerosol using water-condensation
544 technology, *J. Aerosol Sci.*, 36, 866–880, 2005.

545 Kim, S., Jaques, P. A., Chang, M. C., Barone, T., Xiong, C., Friedlander, S. K., and Sioutas, C.:
546 Versatile aerosol concentration enrichment system (VACES) for simultaneous in vivo and in vitro

547 evaluation of toxic effects of ultrafine, fine and coarse ambient particles – Part II: field evaluation,
548 J. Aerosol Sci., 32, 1299–1314, 2001.

549 Kreisberg, N. M., Spielman, S. R., Eiguren-Fernandez, A., Hering, S. V., Lawler, M. J., Draper,
550 D. C., and Smith, J. N.: Water condensation-based nanoparticle charging system: Physical and
551 chemical characterization, Aerosol Sci. Technol., 52, 1167–1177, 2018.

552 Lelieveld, J., Evans, J. S., Fnais, M., Giannadaki, D., and Pozzer, A.: The contribution of outdoor
553 air pollution sources to premature mortality on a global scale, Nature, 525, 367–371, 2015.

554 Liu, P. S. K., Deng, R., Smith, K. A., Jayne, J. T., Williams, L. R., Canagaratna, M. R., Moore,
555 K., Onasch, T. B., Worsnop, D. R., and Deshler, T.: Transmission Efficiency of an Aerodynamic
556 Focusing Lens System: Comparison of Model Calculations and Laboratory Measurements for the
557 Aerodyne Aerosol Mass Spectrometer, Aerosol Sci. Technol., 41, 721–733, 2007.

558 [Ma, X., Zangmeister, C. D., Gigault, J., Mulholland, G. W., and Zachariah, M. R.: Soot aggregate](#)
559 [restructuring during water processing. J. Aerosol Sci., 66, 209–219, 2013.](#)

560 Middlebrook, A. M., Bahreini, R., Jiménez, J. L., and Canagaratna, M. R.: Evaluation of
561 composition-dependent collection efficiencies for the Aerodyne aerosol mass spectrometer using
562 field data, Aerosol Sci. Technol. 46, 258–271, 2012.

563 Ng, N. L., Herndon, S. C., Trimborn, A., Canagaratna, M. R., Croteau, P. L., Onasch, T. B.,
564 Sueper, D., Worsnop, D. R., Zhang, Q., Sun, Y. L., and Jayne, J. T.: An Aerosol Chemical
565 Speciation Monitor (ACSM) for Routine Monitoring of the Composition and Mass Concentrations
566 of Ambient Aerosol, Aerosol Sci. Technol., 45, 780–794, 2011.

567 Onasch, T. B., Trimborn, A., Fortner, E. C., Jayne, J. T., Kok, G. L., Williams, L. R., Davidovits,
568 P., and Worsnop, D. R.: Soot Particle Aerosol Mass Spectrometer: Development, Validation, and
569 Initial Application, Aerosol Sci. Technol., 46, 804–817, 2012.

570 Pan, M., Eiguren-Fernandez, A., Hsieh, H., Afshar-Mohajer, N., Hering, S. V., Lednický, J., Hung
571 Fan, Z., and Wu, C. Y.: Efficient collection of viable virus aerosol through laminar-flow, water-
572 based condensational particle growth, J Appl. Microbiol., 120, 805–815, 2016.

573 Pope, C. A., and Dockery, D. W.: Health Effects of Fine Particulate Air Pollution: Lines that
574 Connect, J. Air & Waste Manage. Assoc., 56, 709–742, 2006.

575 Saarikoski, S., Carbone, S., Cubison, M. J., Hillamo, R., Keronen, P., Sioutas, C., Worsnop, D. R.,
576 and Jimenez, J. L.: Evaluation of the performance of a particle concentrator for online
577 instrumentation, Atmos. Meas. Tech., 7, 2121–2135, 10.5194/amt-7-2121-2014, 2014.

578 Stolzenburg, M., ~~N.~~-Kreisberg, N., and ~~S.~~-Hering, S.: Atmospheric size distributions measured by
579 differential mobility optical particle size spectrometry, Aerosol Sci. Technol., 29, 402–418, 1998.

580 Tunved, P., Hansson, H. C., Kerminen, V. M., Strom, J., Maso, M. D., Lihavainen, H., Viisanen,
581 Y., Aalto, P. P., Komppula, M., and Kulmala, M.: High natural aerosol loading over boreal forests,
582 Science, 312, 261–263, 2006.

583 [Willis, M. D., Lee, A. K. Y., Onasch, T. B., Fortner, E. C., Williams, L. R., Lambe, A. T.,](#)
584 [Worsnop, D. R., and Abbatt, J. P. D.: Collection efficiency of the soot-particle aerosol mass](#)
585 [spectrometer \(SP-AMS\) for internally mixed particulate black carbon, *Atmos. Meas. Tech.*, 7,](#)
586 [4507–4516, 2014.](#)

587 Zauscher, M. D., Moore, M. J., Lewis, G. S., Hering, S. V., and Prather, K. A.: Approach for
588 measuring the chemistry of individual particles in the size range critical for cloud formation, *Anal.*
589 *Chem.*, 83, 2271–2278, 2011.

590

591

Table 1. Approximate temperature and flow settings for the ADIc experiments presented in this study. ADI = Aerosol Dynamics Inc., ARI = Aerodyne Research, Inc., FMI = Finnish Meteorological Institute. Tcon, Tini, Tmod and Tnoz are the operating temperatures for the conditioner, initiator, moderator and focusing nozzle, respectively. AN, AS, DOS are abbreviations for ammonium nitrate, ammonium sulfate and dioctyl sebacate, respectively.

Test site	ADI	ADI	ADI	ARI	ARI	FMI	FMI	FMI
Prototype No.	1	2	2	1	1	2	2	2
Test type	Lab	Lab	Lab	Lab	Field	Lab	Field	Field
Measured parameters/ species	Particle number and size	Particle number	Particle number and size	AN, AS	Chemical composition and size	AN, AS, DOS and particle size	Chemical composition	Chemical composition and size
Tcond (°C)	5	5	6	5	5	6	10	10
Tinit (°C)	26	26	31	26	26	31	31	31
Tmod (°C)	10	10	8	10	10	8	13	13
Tnoz(°C)	30	30	35	30	30	35	35	35
Tout (°C)	35	35	35	n/a	n/a	35	35	35
Sample Flow (L min⁻¹)	1.0	1.0	1.5	0.9	0.9	1.7	1.0	1.7
Output Flow (L min⁻¹)	0.12	0.11	0.11	0.08	0.08	0.08	0.08	0.08
Theoretical CF	8.3	9.1	13.6	11.3 ^a / 12.6 ^b	11.3	21.3	12.5	21.3

^a AN, ^b AS

600

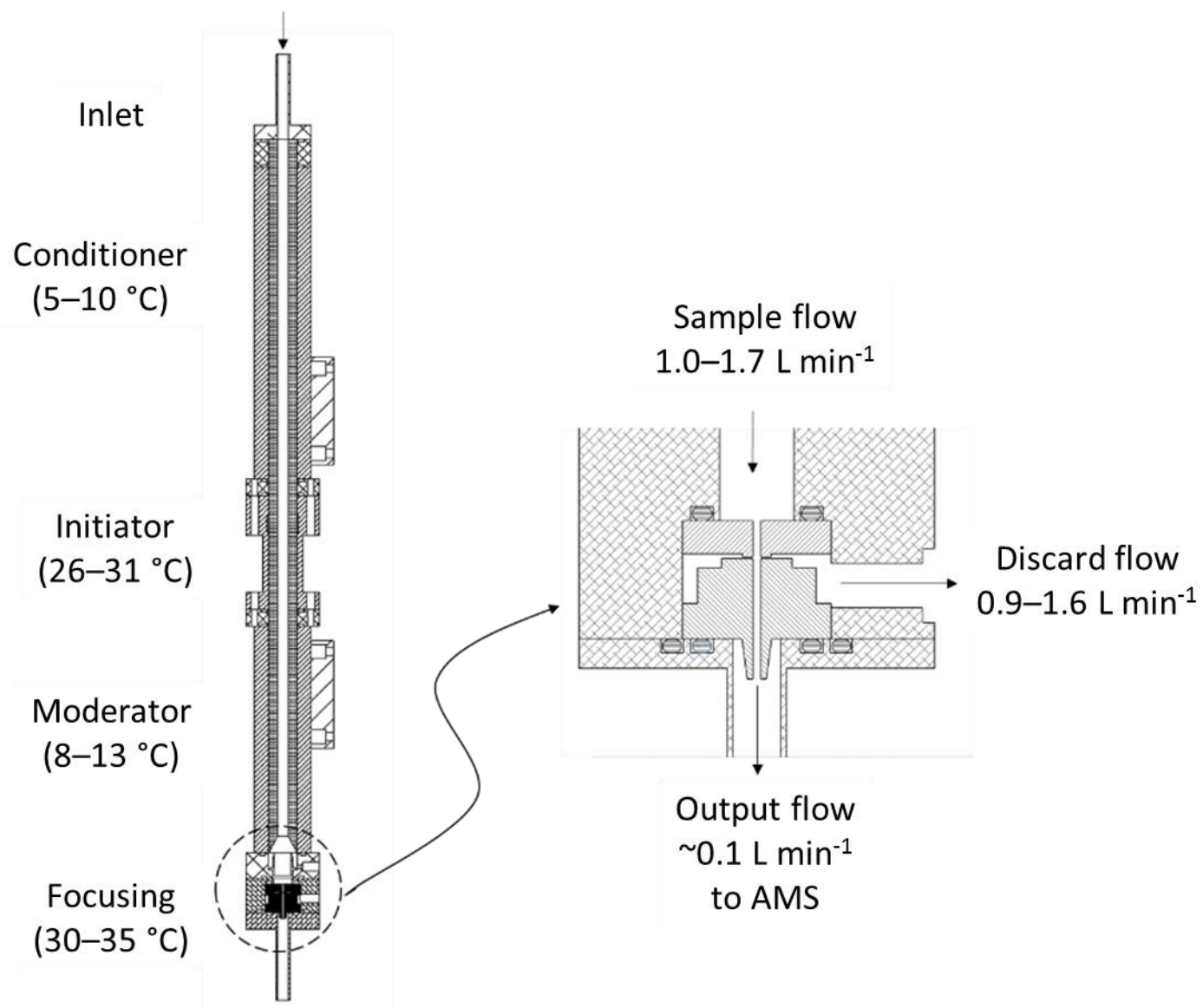
Table 2. Measured and theoretical concentration factors (CFs) for ammonium nitrate (AN) and ammonium sulfate (AS) obtained in the laboratory tests.

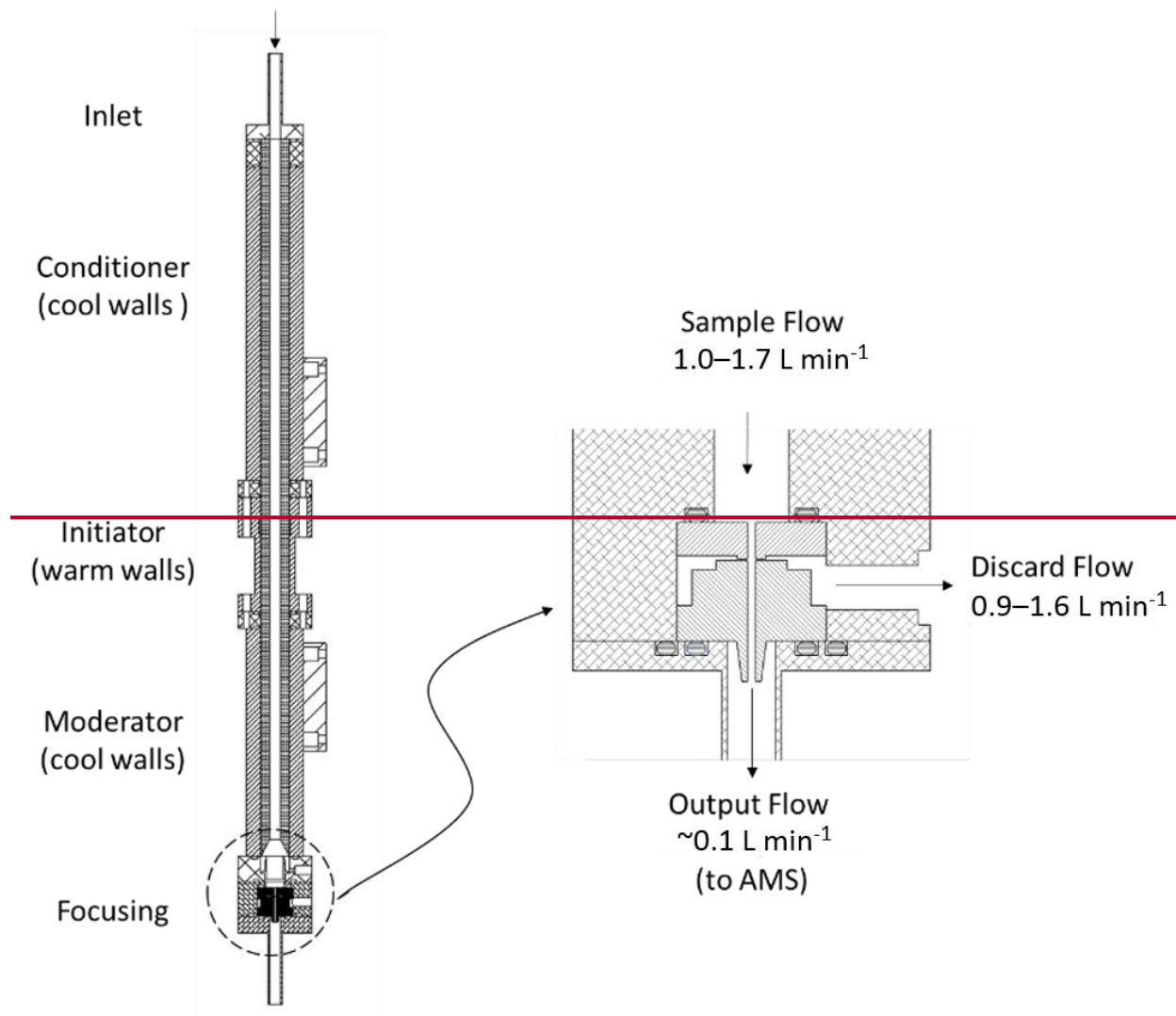
Material	Measured species	Measured CF	Theoretical CF	Measured/ Theoretical CF
AS	Particle number	7.4	8.3	0.89
	Particle number	11.9	13.6	0.88
	Ammonium	11.2	12.6	0.89
	Sulfate	11.3	12.6	0.89
AN	Ammonium	10.6	11.3	0.94
	Nitrate	10.6	11.3	0.94

605 **Table 3.** Measured and theoretical concentration factors, ~~and average mass loadings~~ in ambient measurements at ARI. The measured CF was calculated from the ratio of Q-AMS+ADIC to HR-AMS mass loadings. In the bypass line the sample was not concentrated. The theoretical CF was calculated from the ADIC discard flow rate and the Q-AMS inlet flow rate (see text for details).

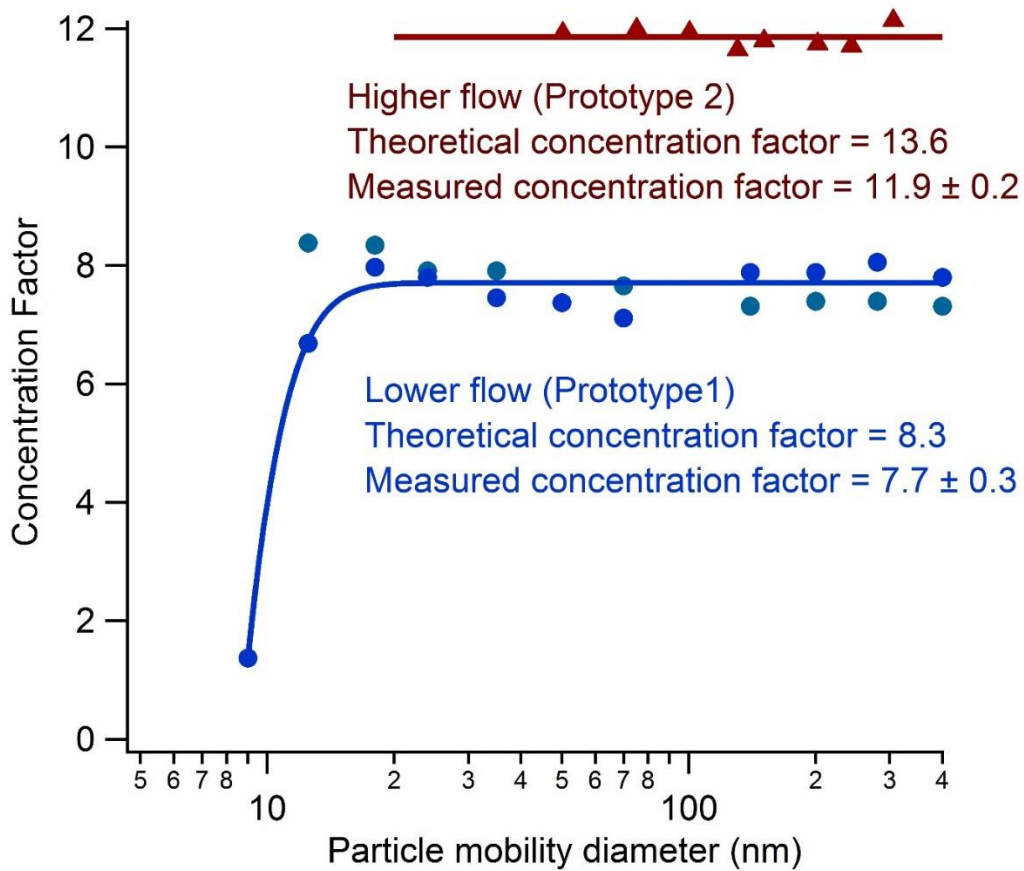
		Through ADIC	Bypass
Measured CF	Organics	6.1 ± 0.8	0.7 ± 0.06
	Sulfate	9.7 ± 1.5	1.0 ± 0.1
	Nitrate	9.1 ± 1.1	1.0 ± 0.1
	Ammonium	12.7 ± 1.9	1.3 ± 0.4
Theoretical CF		10.5 ± 0.3	1.0

610

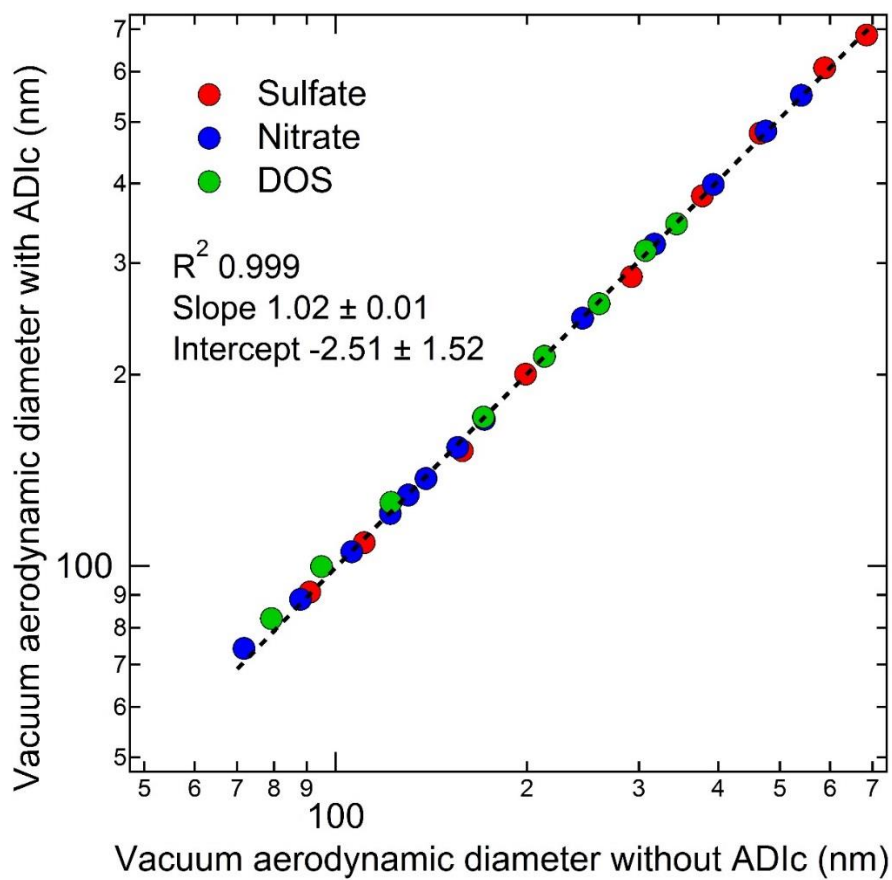




620 **Figure 1.** Schematic of the Aerosol Dynamics Inc. concentrator (ADIC) with enlargement of the focusing nozzle.



625 **Figure 2.** Size dependent concentration factor for the ADIc for higher (triangles) and lower (circles) flow regimes as a function of particle size. The red line indicates the average of the higher flow data. The blue line is a guide for the eye. Data are from two different prototype instruments, as indicated.



630

Figure 3. Particle size measured with an SP-AMS for 70–700 nm particles (vacuum aerodynamic diameter) of sulfate, nitrate and organics (from DOS) with and without concentration by the ADIc. Corresponding mobility diameters were 30–340 nm.

635

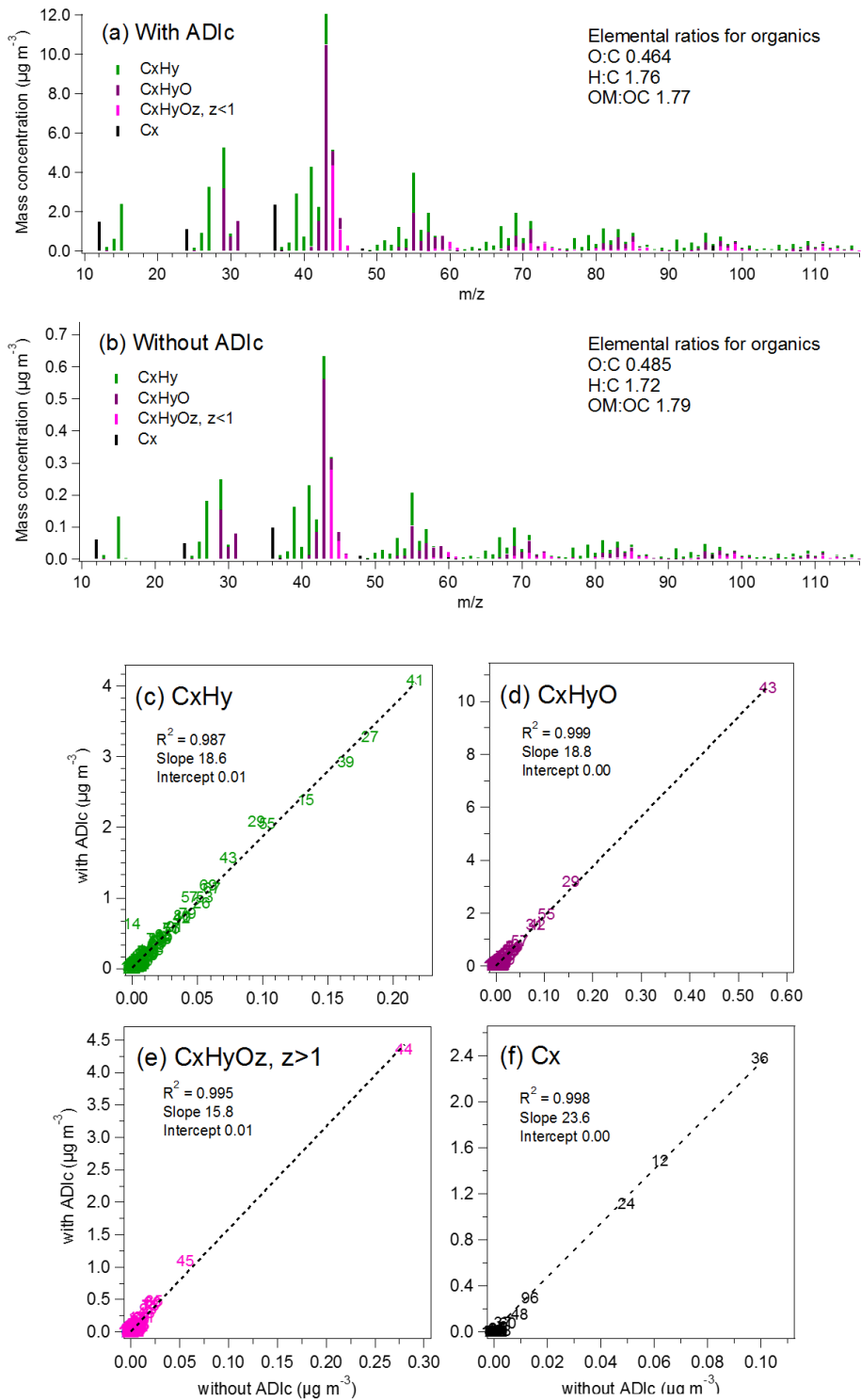


Figure 4. Mass spectra for ambient organics and rBC measured with and without ADIc (a–b) and the correlation of AMS fragment families (c–f) at SMEAR III, Helsinki. Theoretical concentration factor was 21.3.

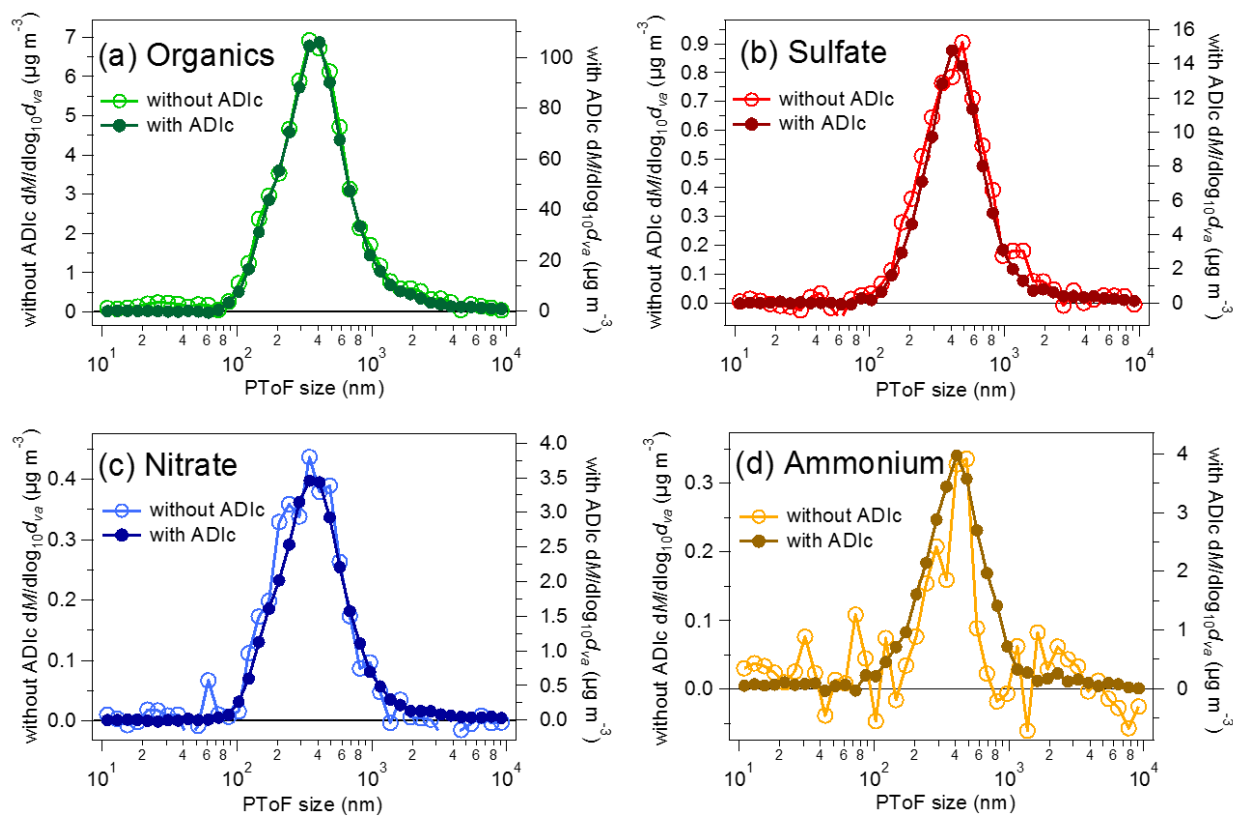
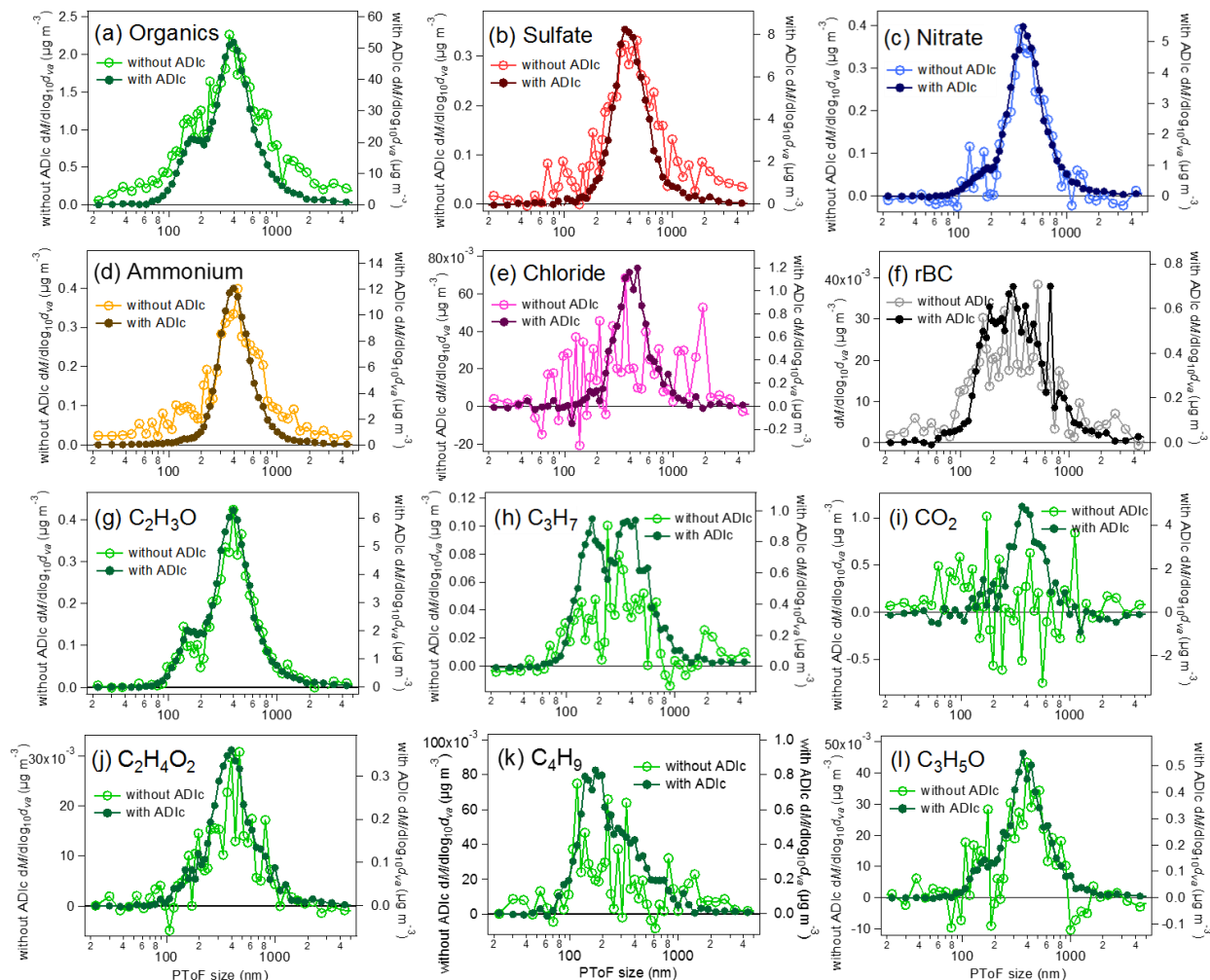


Figure 5. Mass size distributions measured without (left axis) and with (right axis) the ADlc for organics (a), sulfate (b), nitrate (c) and ammonium (d) in UMR mode at SMEAR III. Sampling time for each size distribution was 70 minutes with the ADlc and 70 minutes without the ADlc. The theoretical concentration factor was 21.3.



650 **Figure 6.** Mass size distributions measured without (left axis) and with the ADIc (right axis) for organics (a), sulfate (b), nitrate (c), ammonium (d), chloride (e), rBC (f), C_2H_3O (g), C_3H_7 (h), CO_2 (i), $C_2H_4O_2$ (j), C_4H_9 (k) and C_3H_5O (l) in HR mode at SMEAR III. Sampling time for each size distribution was 70 minutes without and 70 minutes with the ADIc. Theoretical concentration factor was 21.3.

655

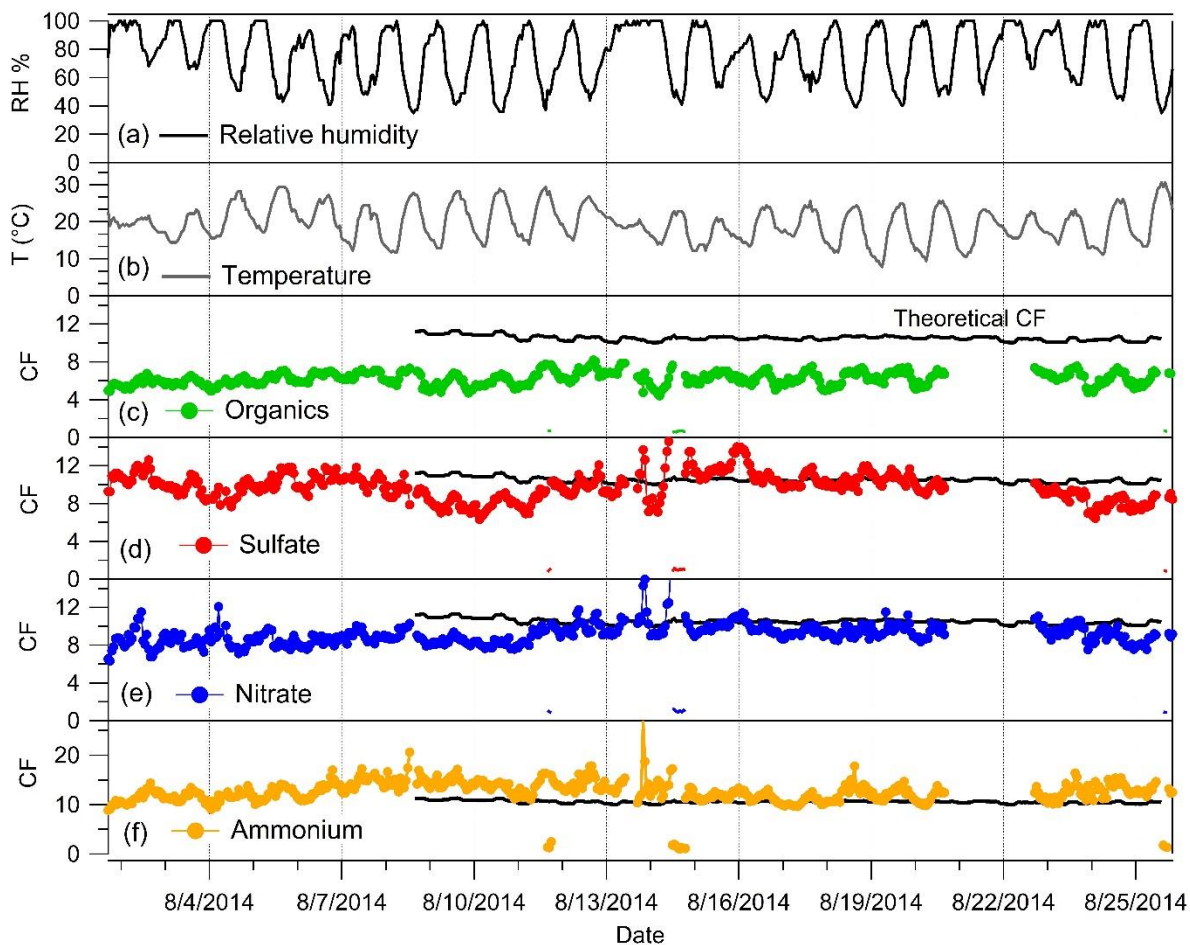


Figure 7. Ambient measurements at ARI showing ambient relative humidity (a), ambient temperature (b) and measured CFs for organics (c), sulfate (d), nitrate (e), and ammonium (f). The theoretical CF is shown with the black line in (c) – (f).

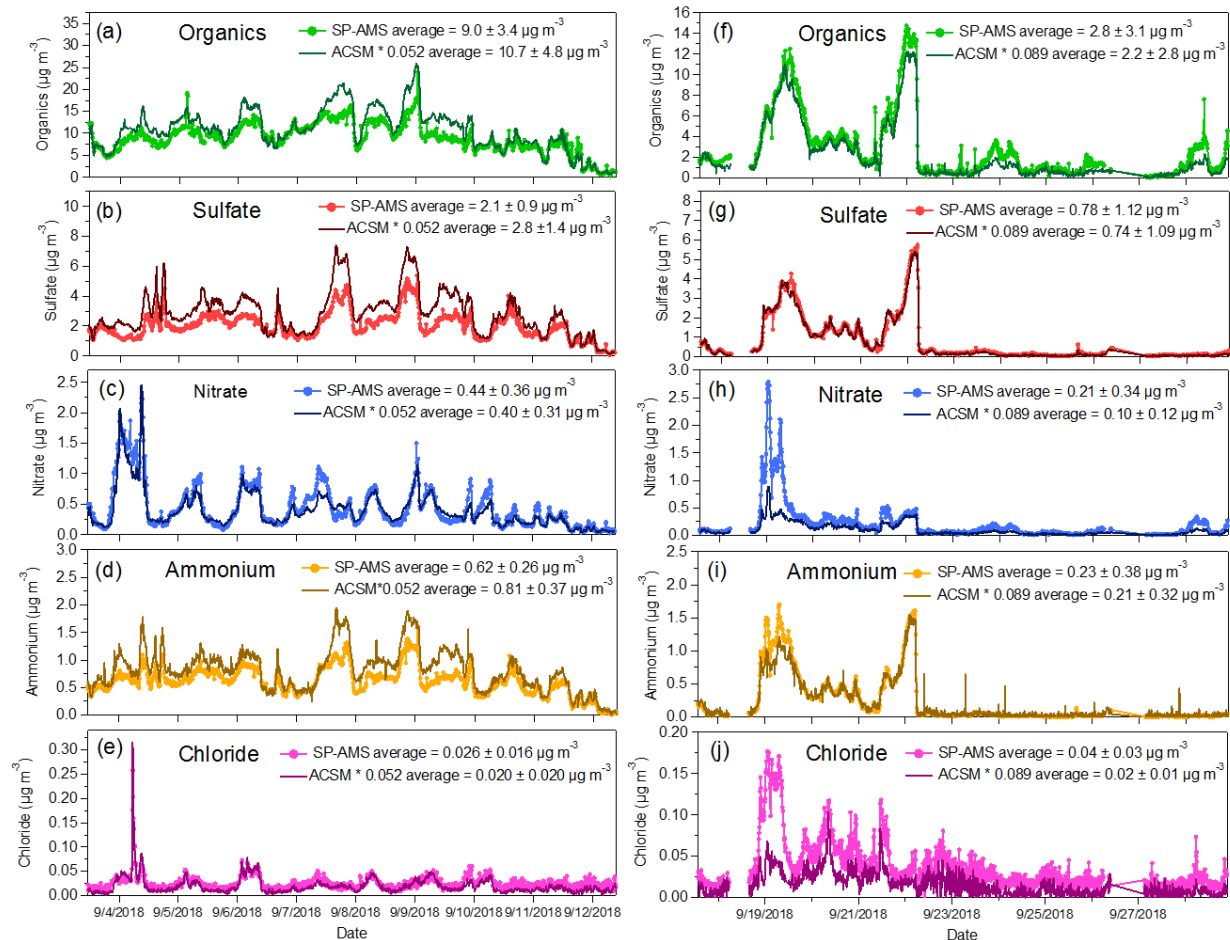


Figure 8. Ambient measurements at SMEAR III showing the mass loadings for organics (a, f), sulfate (b, g), nitrate (c, h), ammonium (d, i), and chloride (e, j) measured with the SP-AMS and the ACSM+ADIC in high flow (a–e) and low flow (f–j) regimes. ACSM+ADIC data was corrected for CF as described in the text. Spikes in the time series of ammonium in the ACSM are likely related to the detection of small air bubbles in the ACSM that affect the measured ammonium concentration.

670

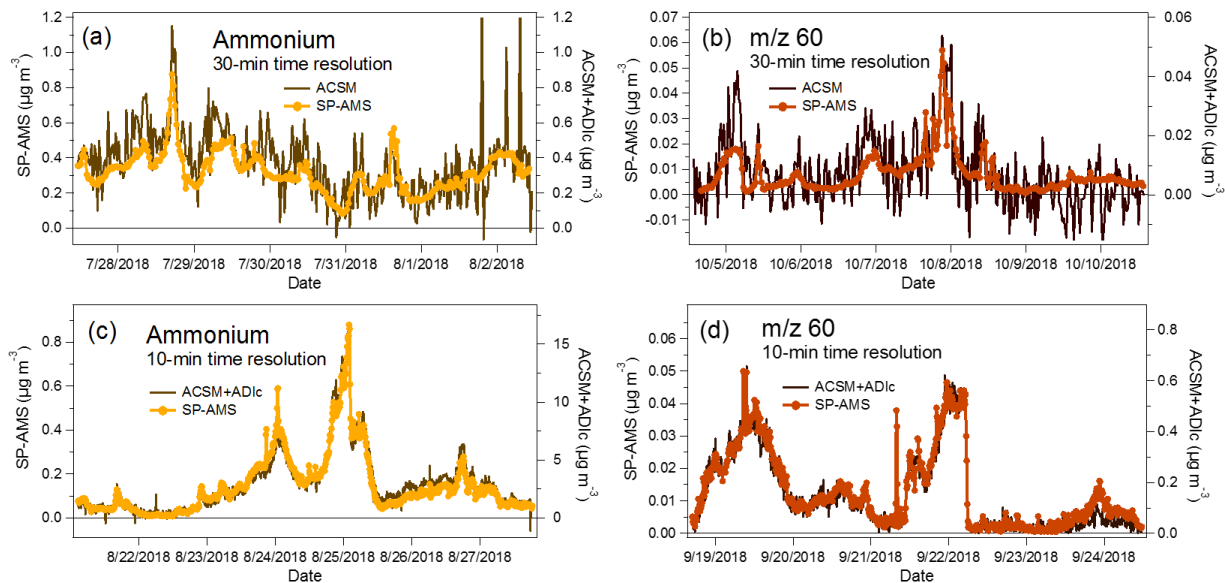


Figure 9. Time series of ammonium and m/z 60 with 30-min time resolution with ACSM and SP-AMS (a-b) and 10-min time resolution with SP-AMS and ACSM+AD1c (c)-(d) at SMEAR III

Laboratory and field evaluation of the Aerosol Dynamics Inc. concentrator (ADIC) for aerosol mass spectrometry

Sanna Saarikoski¹, Leah R. Williams², Steven R. Spielman³, Gregory S. Lewis³, Arantzazu Eiguren-Fernandez³, Minna Aurela¹, Susanne V. Hering³, Kimmo Teinilä¹, Philip Croteau², John T. Jayne², Thorsten Hohaus^{2,+}, Douglas R. Worsnop², Hilkka Timonen¹

¹ Atmospheric Composition Research, Finnish Meteorological Institute, Helsinki, Finland

² Center for Aerosol and Cloud Chemistry, Aerodyne Research, Inc., Billerica, MA, USA

³ Aerosol Dynamics Inc., Berkeley, CA, USA

⁺ Now at Institute of Energy and Climate Research, IEK-8: Troposphere, Forschungszentrum Juelich GmbH, Juelich, Germany

Supplemental Information

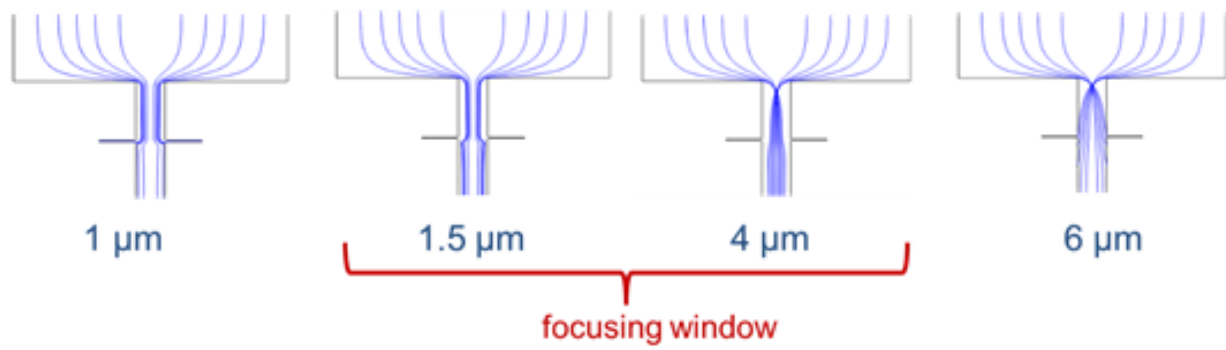


Figure S1. Calculated particle trajectories for different particle sizes entering the focusing nozzle of the ADIc. Scale is expanded radially for better visualization.

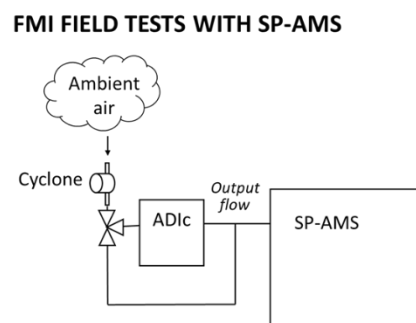
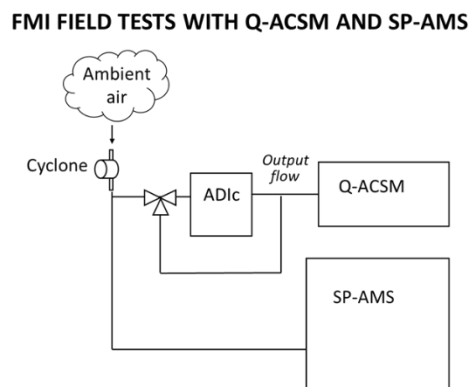
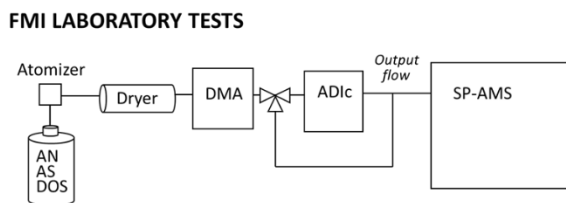
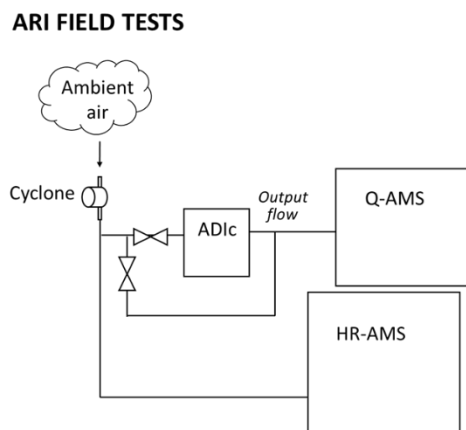
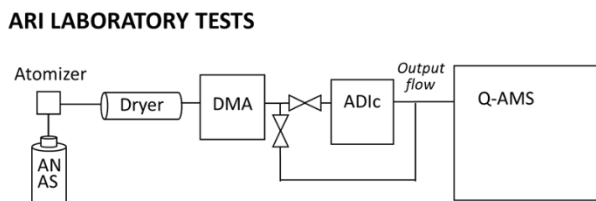
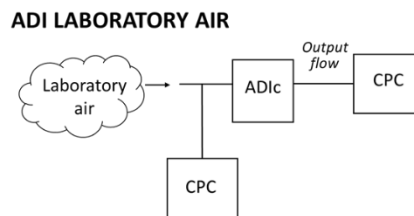
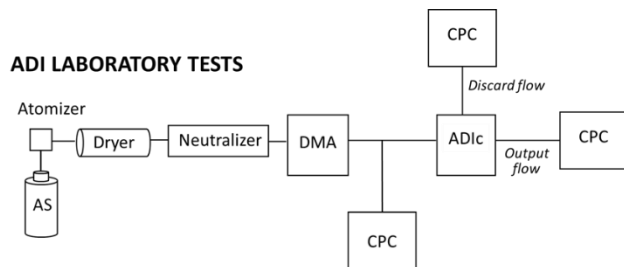


Figure S2. Diagrams for the instrumental set-ups used in the laboratory and field tests at Aerosol Dynamics Inc. (ADI), Aerodyne Research, Inc. (ARI) and Finnish Meteorological Institute (FMI).

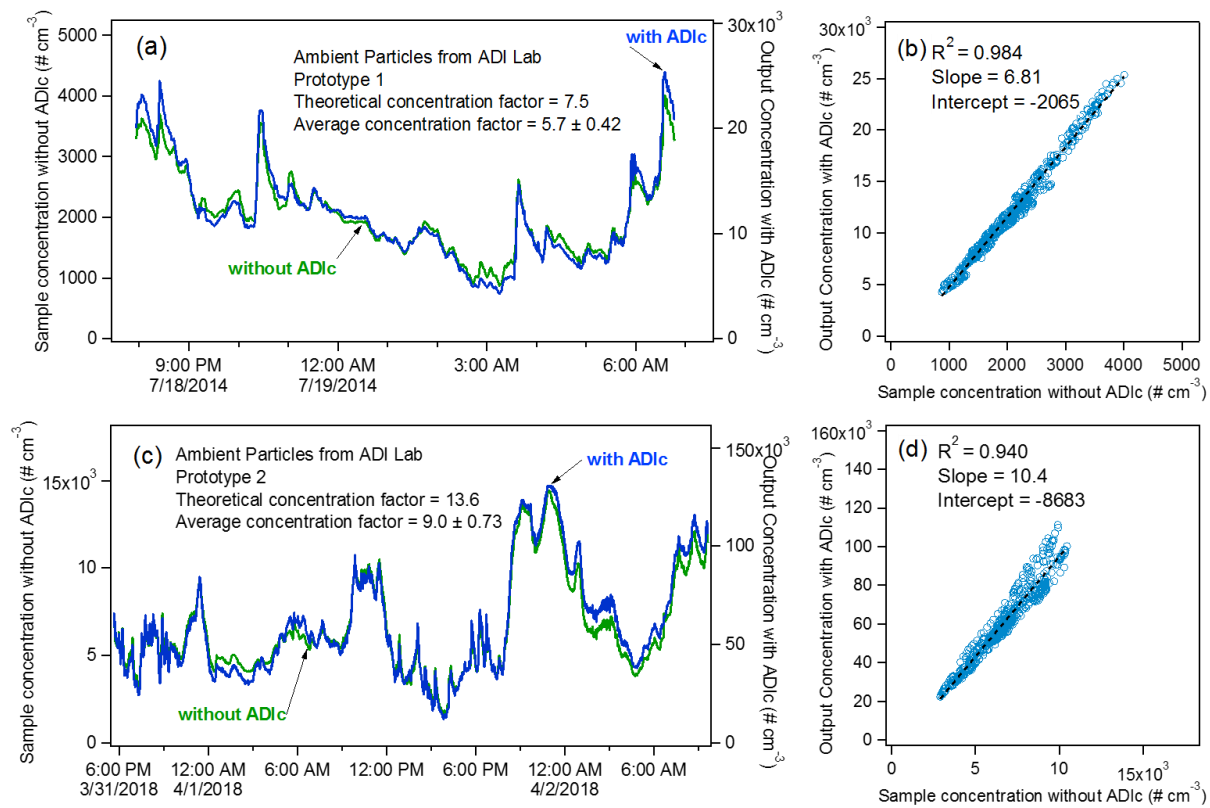


Figure S3. Particle number concentrations in the ADIc sample and output flows while sampling laboratory air shown as time series (a, c) and as correlation plots (b, d). Prototype 1 was operating at low flow (a–b) and prototype 2 at high flow (c–d).

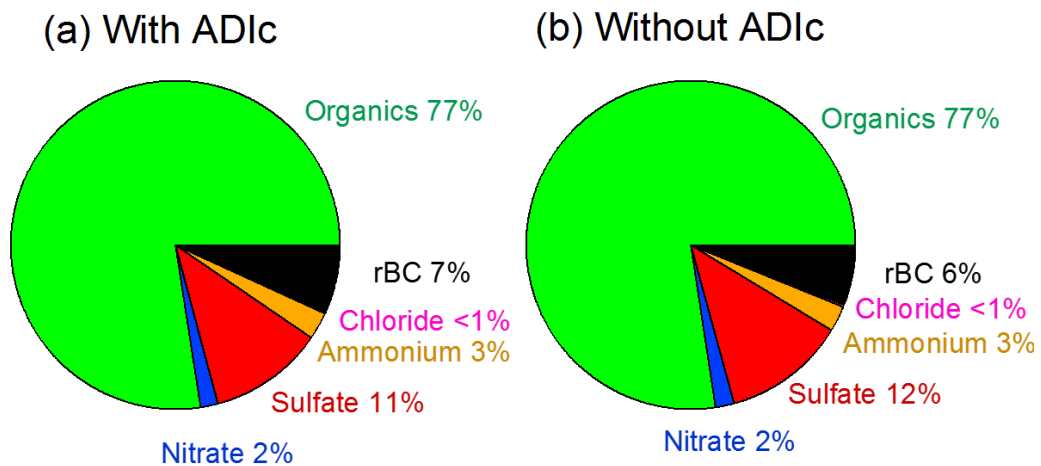


Figure S4. Chemical composition of particles with the ADIc (a) and without the ADIc (b) measured with the SP-AMS at SMEAR III. Sampling time was 70 minutes with the ADIc and 70 minutes without the ADIc. The theoretical concentration factor was 21.3.

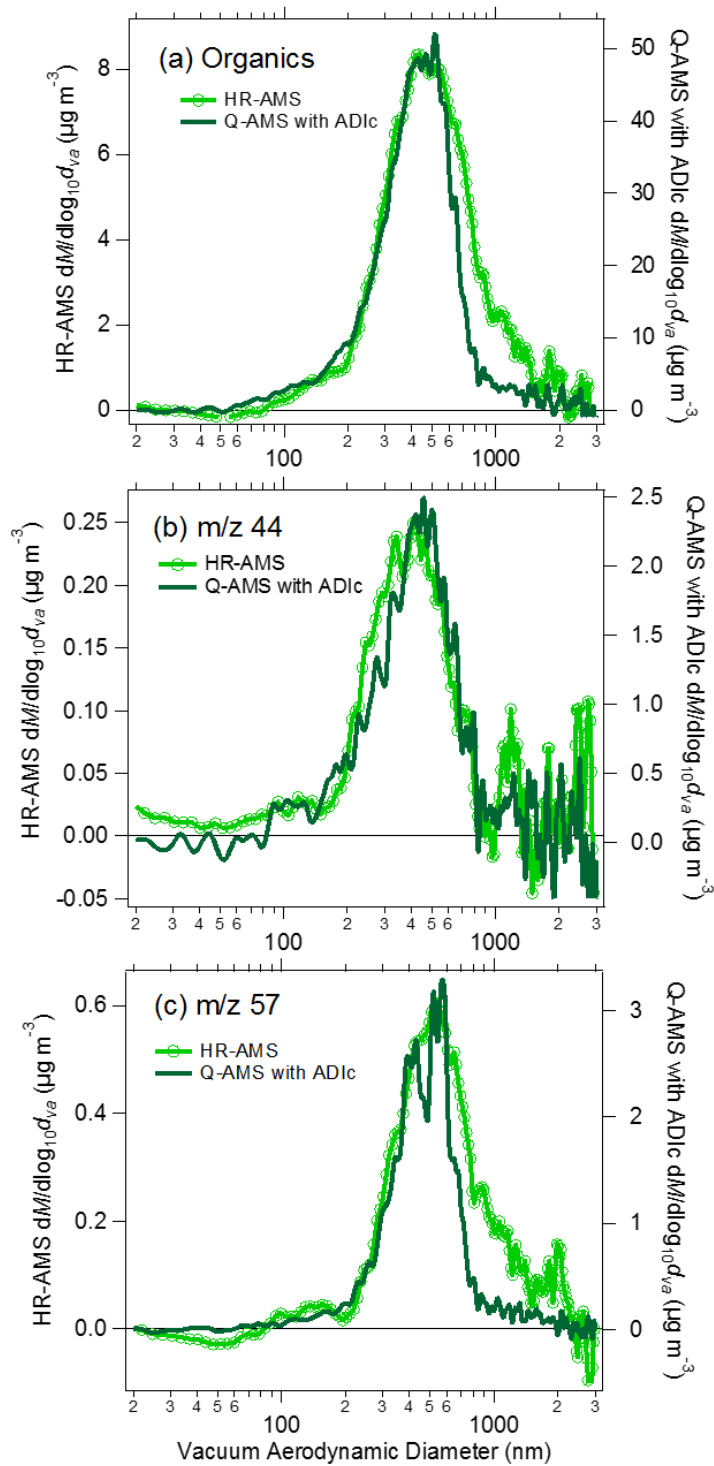


Figure S5. Size distributions for organics (a), m/z 44 (b) and m/z 57 (c) from the HR-AMS in bypass (without the ADIc) and the Q-AMS behind the ADIc demonstrating different size cutoffs in the aerodynamic lenses >700 nm in the two instruments.